(4)

NORTH CAROLINA A&T STATE UNIVERSITY

Greensboro, NC 27411

School of Engineering

FINAL REPORT

"REFINED TEST METHODS IN EVALUATING BRITTLE
MATERIAL FRACTURE STRENGTHS "

Contract No. N00019-79-C-0574

December 2, 1982

"Approved for Public Release--Distribution Unlimited"

William J. Craft

Principal Investigator

Professor

Mechanical Engineering

(919) 379-7549

George J. Filatovs

Co-Investigator
Professor
Mechanical Engineering
(919) 379-7620
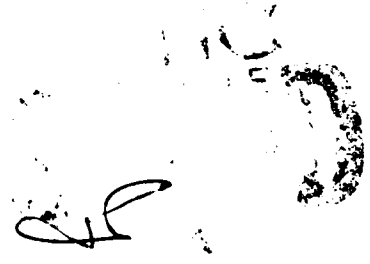
DISCLAIMER NOTICE

THIS DOCUMENT IS BEST QUALITY
PRACTICABLE. THE COPY FURNISHED
TO DTIC CONTAINED A SIGNIFICANT
NUMBER OF PAGES WHICH DO NOT
REPRODUCE LEGIBLY.

NORTH CAROLINA A&T STATE UNIVERSITY

Greensboro, NC 27411

School of Engineering

FINAL REPORT

"REFINED TEST METHODS IN EVALUATING BRITTLE
MATERIAL FRACTURE STRENGTHS"

Contract No. N00019-79-C-0574

December 2, 1982

William J. Craft

Principal Investigator

Professor

Mechanical Engineering

(919) 379-7549

George J. Filatovs

Co-Investigator
Professor
Mechanical Engineering
(919) 379-7620

REPORT DOCUMENTATION PAGE		READ INSTRUCTIONS BEFORE COMPLETING FORM
1. REPORT NUMBER 340-20209	2. GOVT ACCESSION NO. AD-A133 566	3. RECIPIENT'S CATALOG NUMBER
4. TITLE (and Subtitle) Refined Test Methods in Evaluating Brittle Material Fracture Strengths		5. TYPE OF REPORT & PERIOD COVERED Final
		6. PERFORMING ORG. REPORT NUMBER 340-20209
7. AUTHOR(s) William J. Craft George J. Filatovs		8. CONTRACT OR GRANT NUMBER(s) N00019-79-C-0574
9. PERFORMING ORGANIZATION NAME AND ADDRESS School of Engineering North Carolina A&T State University 312 N Dudley Street Greensboro, NC 27411		10. PROGRAM ELEMENT, PROJECT, TASK AREA & WORK UNIT NUMBERS
11. CONTROLLING OFFICE NAME AND ADDRESS Department of the Navy Naval Air Systems Command Washington, D. C. 20361		12. REPORT DATE December 2, 1982
		13. NUMBER OF PAGES
14. MONITORING AGENCY NAME & ADDRESS(if different from Controlling Office)		15. SECURITY CLASS. (of this report) Unclassified
		15a. DECLASSIFICATION/DOWNGRADING SCHEDULE

16. DISTRIBUTION STATEMENT (of this Report)

Approved for Public Release – Distribution Unlimited

17. DISTRIBUTION STATEMENT (of the abstract entered in Block 20, if different from Report)

18. SUPPLEMENTARY NOTES

19. KEY WORDS (Continue on reverse side if necessary and identify by block number)

Ceramics, Brittle Materials, Alumina, Mullite (MV33), Weibull Parameters, Ceramic Tubes, Torsion, Ceramic Disk, Pressure Loading of Simply Supported Disk.

20. ABSTRACT (Continue on reverse side if necessary and identify by block number)

In this report entitled, "Refined Test Methods In Evaluating Brittle Material Fracture Strengths," Contract No. N00019-79-C-0574, is a follow-up of the work done under the previous contract, entitled, "Fracture Prediction in Brittle Materials,".

In the former contract, an analytical system was devised to generate fracture data based on: (1) conversion of triaxial fracture data to a

(Question 20 continued)

single variable, ϕ, the angle on the fracture surface from point of fracture to the n=(1,1,1) direction, (2) the creation of a simple test procedure and specimen design to find a variety of points on the fracture surface, and (3) the design of experiments to employ this testing system. In the first contract, both alumina and mullite specimens were tested in four-point loading and these results were reduced to a Weibull distribution by determination of the two-parameter coefficients.

In this contract, a torsion test method and apparatus were designed and implemented. Both alumina and mullite specimens, the same geometry as was used in the four-point bend test of the previous contract were loaded in torsion to failure at another angle on the fracture surface, or at $\phi=90°$ to the n=(1,1,1) direction. The results are given for alumina and mullite tests.

Finally, a general test utilizing 'thick' disks of each material is described. The literature seems to lack a simple reliable disk test for which a simple stress distribution is readily available. The test produces an axially symmetric state of stress but one that embodies a variety of orientations to the n=(1,1,1) direction. The use of a hydraulic ram gives rise to an easily predictable stress field. The expected Weibullian scatter was detected in both alumina and mullite specimens which were tested in both as-cast and ground conditions. No problems attributable to lack of flatness in these low-strain-to-failure materials were detected in as-cast samples. The alumina samples tended not to show fracture propagation throughout the thickness while the mullite samples did demonstrate this behavior. Because it was sometimes difficult to determine precisely what pressure produced incipient cracking in alumina, a differential current detector employing a conductive brittle coating has been proposed--the coating brittleness being chosen to match the specimen strain-to-failure.

Abstract

In this report entitled, "Refined Test Methods In Evaluating Brittle Material Fracture Strengths," Contract No. N00019-79-C-0574, is a follow-up of the work done under NAVAIR No. N00019-78-C-0520, entitled, "Fracture Prediction in Brittle Materials.".

In the former contract, an analytical system was devised to generate fracture data based on: (1) conversion of triaxial fracture data to a single variable, ϕ, the angle on the fracture surface from point of fracture to the $\hat{n}=(1,1,1)$ direction, (2) the creation of a simple test procedure and specimen design to find a variety of points on the fracture surface, and (3) the design of experiments to employ this testing system. In the first contract, both alumina and mullite specimens were tested in four-point loading and these results were reduced to a Weibull distribution by determination of the two-parameter coefficients.

In this contract, a torsion test method and apparatus were designed and implemented. Both alumina and mullite specimens, the same geometry as was used in the four-point bend test of the previous contract were loaded in torsion to failure at another angle on the fracture surface, or at ϕ=90 to the $\hat{n}=(1,1,1)$ direction. The results are given for alumina and mullite tests.

Finally, a general test utilizing 'thick' disks of each material is described. The literature seems to lack a simple reliable disk test for which a simple stress distribution is readily available. The test produces an axially symmetric state of stress but one that embodies a variety of orientations to the $\hat{n}=(1,1,1)$ direction. The use of a hydraulic ram gives rise to an easily predictable stress field. The

expected Weibullian scatter was detected in both alumina and mullite specimens which were tested in both as-cast and ground conditions. No problems attributable to lack of flatness in these low-strain-to-failure materials were detected in as-cast samples. The alumina samples tended not to show fracture propagation throughout the thickness while the mullite samples did demonstrate this behavior. Because it was sometimes difficult to determine precisely what pressure produced incipient cracking in alumina, a differential current detector employing a conductive brittle coating has been proposed—the coating brittleness being chosen to match the specimen strain-to-failure.

ACKNOWLEDGEMENT

TABLE OF CONTENTS

TABLE OF GRAPHS

TABLE OF FIGURES

TABLES OF FIGURES (cont.)

TABLE OF TABLES

Chapter 1

THEORY OF THE TORSION TEST

A circular prism. rod. or tube can be subjected to a state of pure torsion along its gage length. Fig. 1.1.
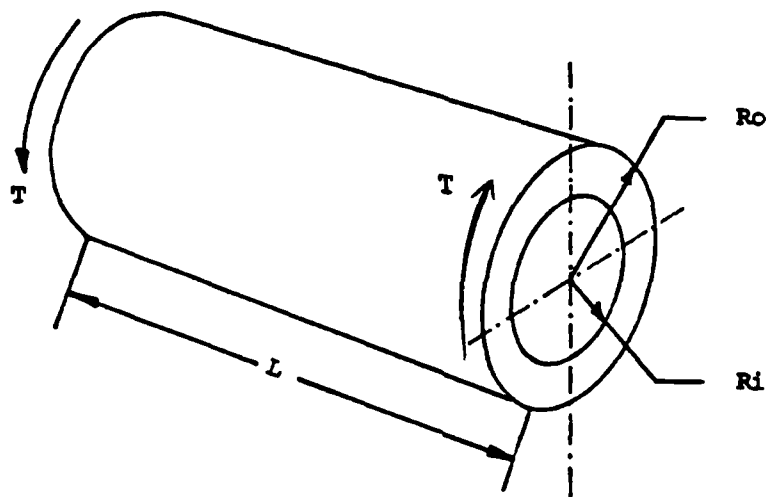
Figure 1.1 Biaxial Stress Envelope for Circular Cross-Section
Tube Subjected to Pure Torsion

The Biaxial stress state depicted by Mohr's circle. Fig. 1.2. is applicable to every point of the specimen if edge effects are neglected. As demonstrated by the results in Chapter 3. the edge effects did not contribute to testing error in a significant way. However. almost some stress concentration is to be expected in any experiment and attempts should be devised to minimize it as with the special end caps and adhesives described in Chapter 2.
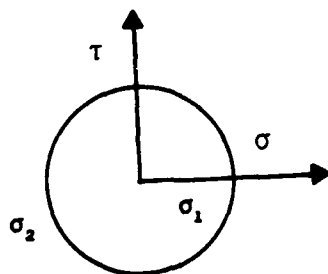
Figure 1.2 Mohr's Circle in Pure Torsion

The probability of failure is:

$$F(T) = 1 - \exp(-Bn)$$

<div align="right">1.1</div>

The risk of fracture or rupture can be expressed easily in integral form since the radial volume element and stress level are simply related. Further, a scalar variable, τ, that is one possible contraction of the stress state torsion is used in the integral to obtain:

$$Bn = Lc \iint \left(\frac{T r}{J} - \sigma_u \right)^m r \, d\theta \, dr$$

where $c = \dfrac{1}{V_{un}(\sigma_o)^m}$, $\tau = \dfrac{Tr}{J}$ and L = the gage length.

<div align="right">1.2</div>
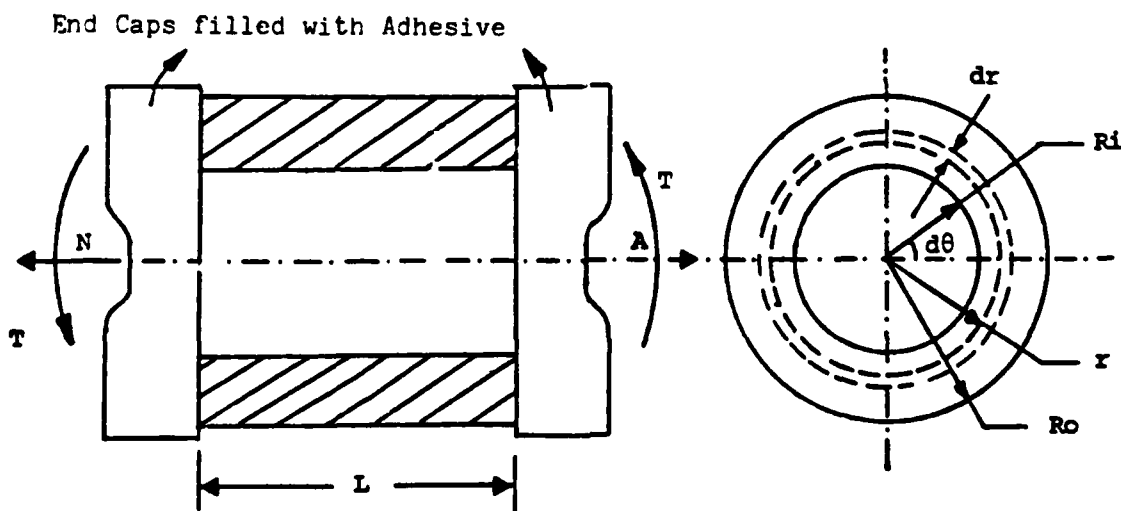
Fig. 1.3 **Pure Torsion for a Circular Cross-Section Tube**

Using the **same** approach as in [1] rods and tubes are separately considered:

(1) <u>Rod (Ri = 0)</u> : Two cases occur;

(a) $0 \leq R_{th} < Ro$; where $R_{th} = \dfrac{\sigma_u J}{T}$, and B_n becomes

$$B_n = \frac{2\pi Lc}{(m+1)\left(\dfrac{T}{J}\right)} \left[r\left(\frac{T\,r}{J} - \sigma_u\right)^{m+1} - \frac{\left(\dfrac{T\,r}{J} - \sigma_u\right)^{m+2}}{\left(\dfrac{T}{J}\right)(m+2)} \right]_{R_{th}}^{Ro} \qquad 1.3$$

(b) $Ro \leq R_{th}$; In this case;

$$B_n = 0. \qquad\qquad 1.4$$

(2) Tube $(Ri \neq 0)$: Three cases occur;

(a) $Ro > R_{th} > Ri$

Bn is expressed by Eq. (1.3)

(b) $0 \leq R_{th} \leq Ri$

Bn is expressed by Eq. (1.3) except the lower limit

of integration is replaced by Ri.

(c) $R_{th} \geq Ro$; in this case;

$$B_n = 0.,$$

Equation (1.3) has the same form as the case of the uniaxial tension
field and can be correlated with either the three-parameter Weibull distri-
bution or the two-parameter distribution in an iterative programming scheme,
similar to UNIAX.FOR. [1]

Any of the scalars, the shear stress, T; the effective tensile
principal stress, $\sigma_1 = T\,r/J$; or the 'biaxial intensity', σ, can be used in
Eq. (1.3) for the study. This intensity might be developed

14

in several ways including the correlation of test results with

1) the most tensile component of the stress tensor or 2) the strain

energy of distortion [2].

In either case, each element is considered to be under a torsional

stress, where $\tau = Tr/J$ is assumed, and the risk of rupture for the whole

specimen is obtained by integrating the risk of rupture of each infinites-

inal element over the gage volume of the specimen. Thus, 1.3 applies.

Under this pure torsion, the stress field $\tau_{rz}=Tr/J$ results from

which the principal direction stresses are:

$$\sigma_1 = \tau_{rz} \quad ; \quad \sigma_2 = -\tau_{rz} \qquad\qquad 1.5$$

Normally the compressive component, σ_2, would be neglected and a

uniaxial stress state, σ_1, would be assumed. In this case $\sigma = \sigma_1 = Tr/J$.

If distortion energy is employed to define σ_1 then under pure torsion:

$$U^1 = \frac{(\sigma_1-\sigma_2)^2 + (\sigma_2-\sigma_3)^2 + (\sigma_3-\sigma_1)^2}{12G}$$

or

$$U^1 = \frac{\sigma_1^2}{2G} \qquad\qquad 1.6$$

For this study, compression was ignored and $\sigma_1 = \tau = Tr/J$

led to 1.3.

15

Chapter 2

DESCRIPTION OF THE TORSION TEST

The torsion test method required the creation of a torsion test loading system designed to operate in conjunction with a standing universal testing machine, Figure 2.1. The actual torsion test fixture designed to accept a specimen between two universal joints, Figure 2.2, was also designed to eliminate all loads except pure torsion.

The pictorial view, Figure 2.3, demonstrates the current configuration in general while the component dimensioned drawings provided detail, Figure 2.4, 5. The experiment was first conceived as one that did not require a locking bar behind each collet. It was found, however, that the experiment was unsuccessful because the hardened collets or chucks slipped before fracture stress was obtained. Naturally, these early tests were conducted on alumina, the stronger of the two materials. The original sleeves, Figure 1.3, were thus machined to allow for a slot and the experiment repeated.

The next problem was one of adhesives. A rough calculation indicated that an elastomer adhesive would need to withstand up to 3000 p.s.i. in shear to sustain a load sufficiently high to fracture alumina. After consultations with 3M adhesive experts a film adhesive -- 3M AF-126-2 -- was selected. Surfaces of both the ceramic and metal sleeve were prepared carefully to permit good bonding. The adhesive was cured as specified and several specimens were tested.

The results of these tests were disappointing and all joints failed at no greater than 25% of the expected alumina fracture torque. Perhaps this problem was caused by (1) use of a 'bad' or degraded batch of adhesive
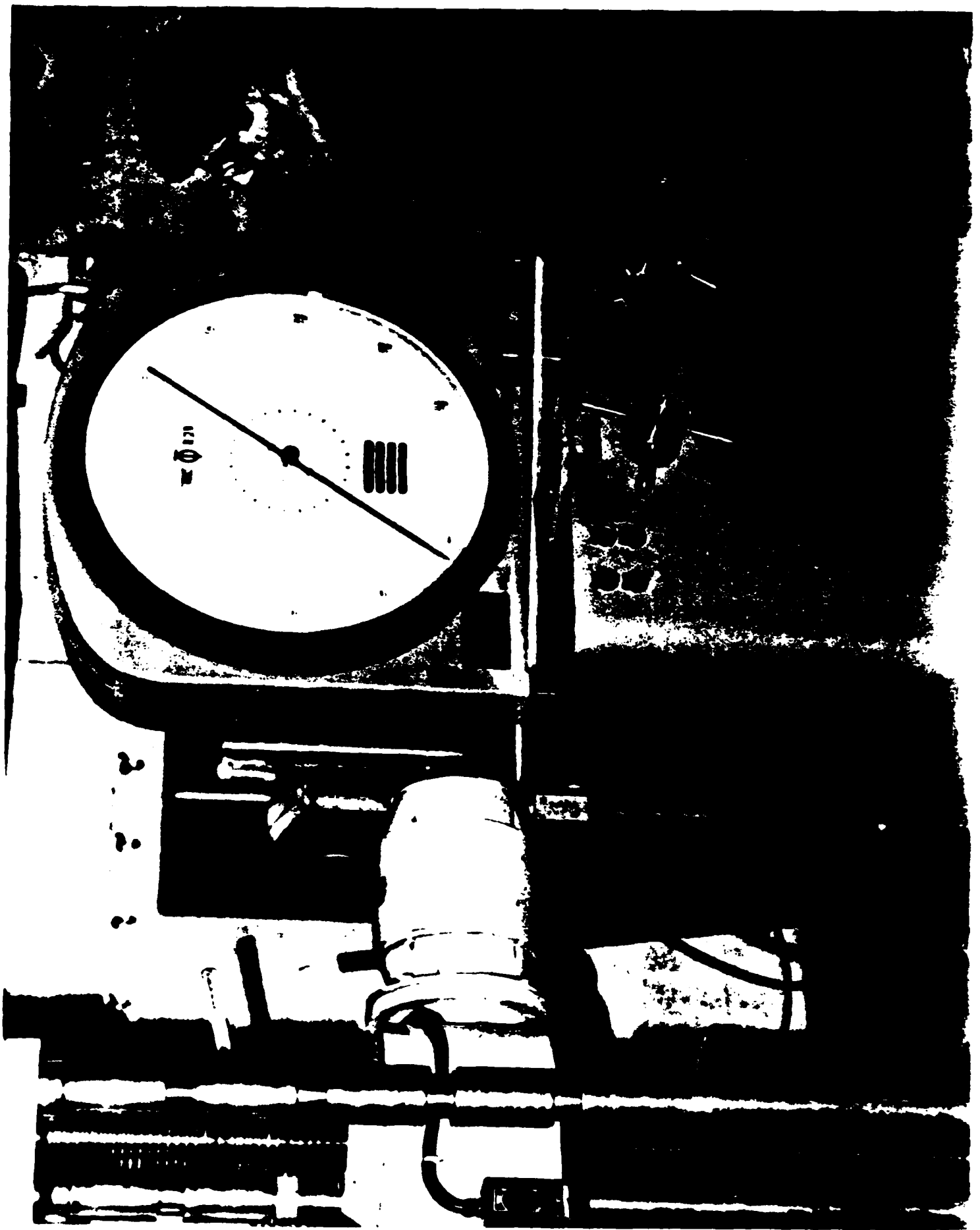
Figure 2.1. Universal Testing Facility

17
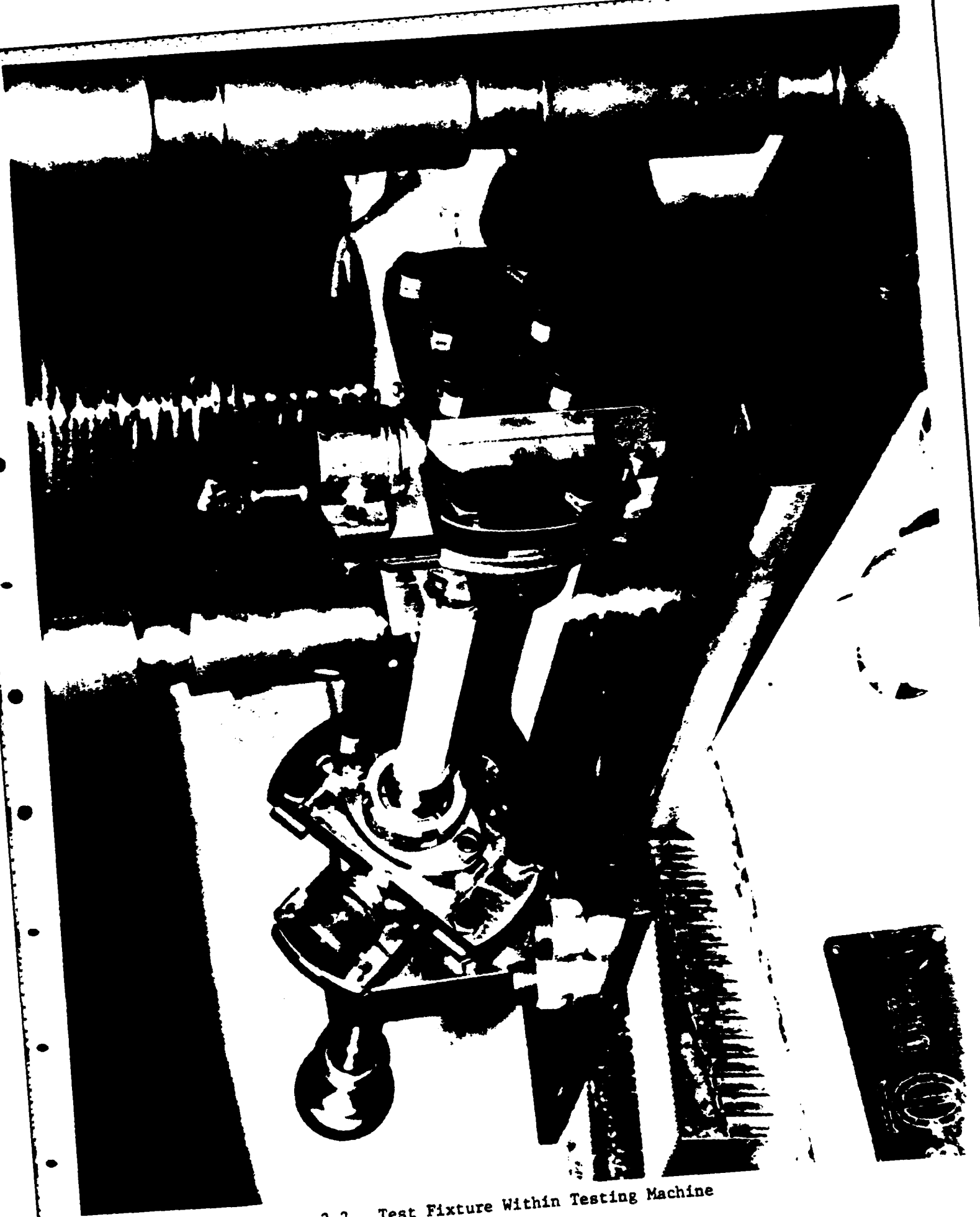
Figure 2-2. Test Fixture Within Testing Machine

To universal
Testing Machine
Lever Axis

Ground Mated
Bearing Surfaces
1¼-Diameter

Type 570 Precision Universal Joint.
Mechanics Type – 4", Heavy.

Stub Collet Holder
and Collet
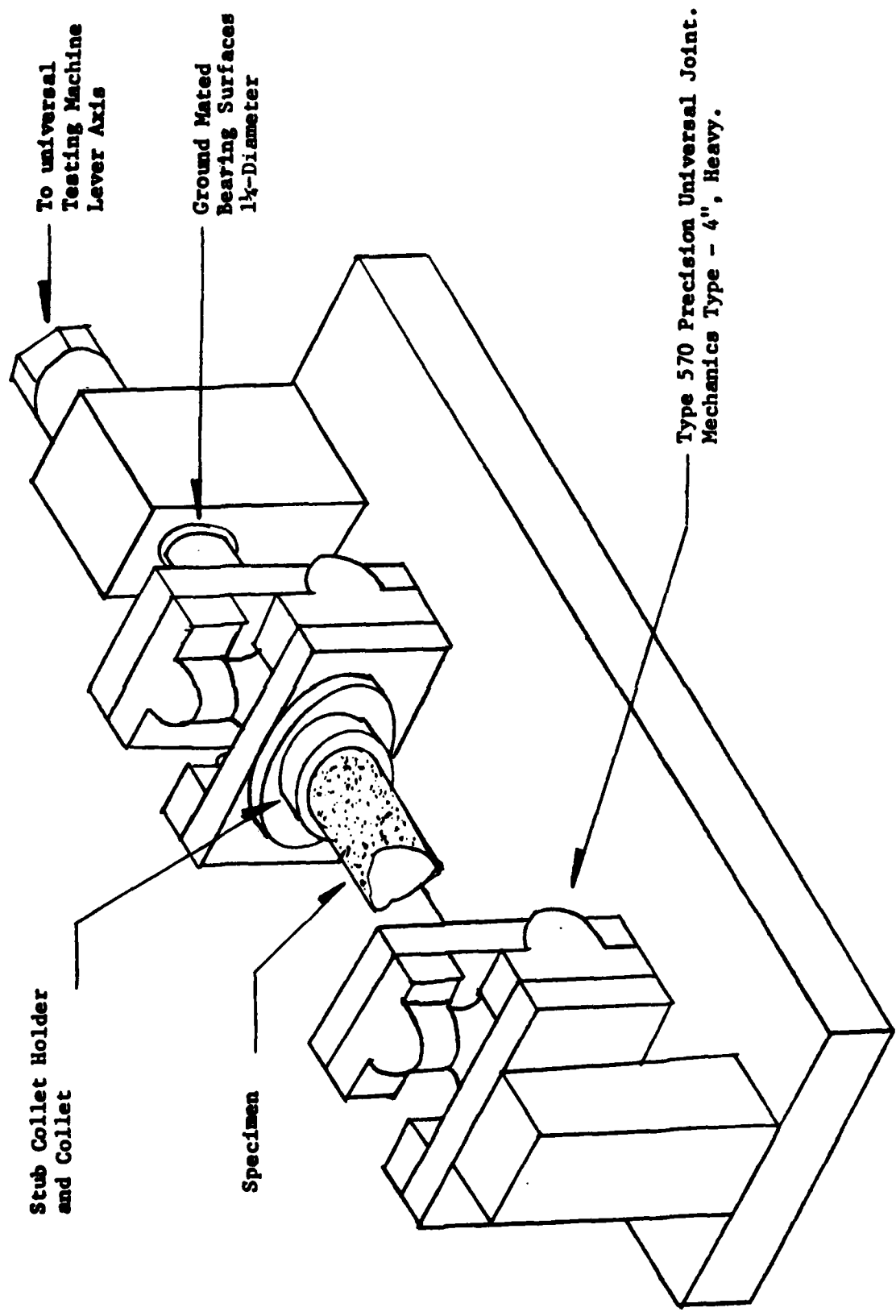
Specimen

Figure 2.3 Torsion Testing Fixture

19
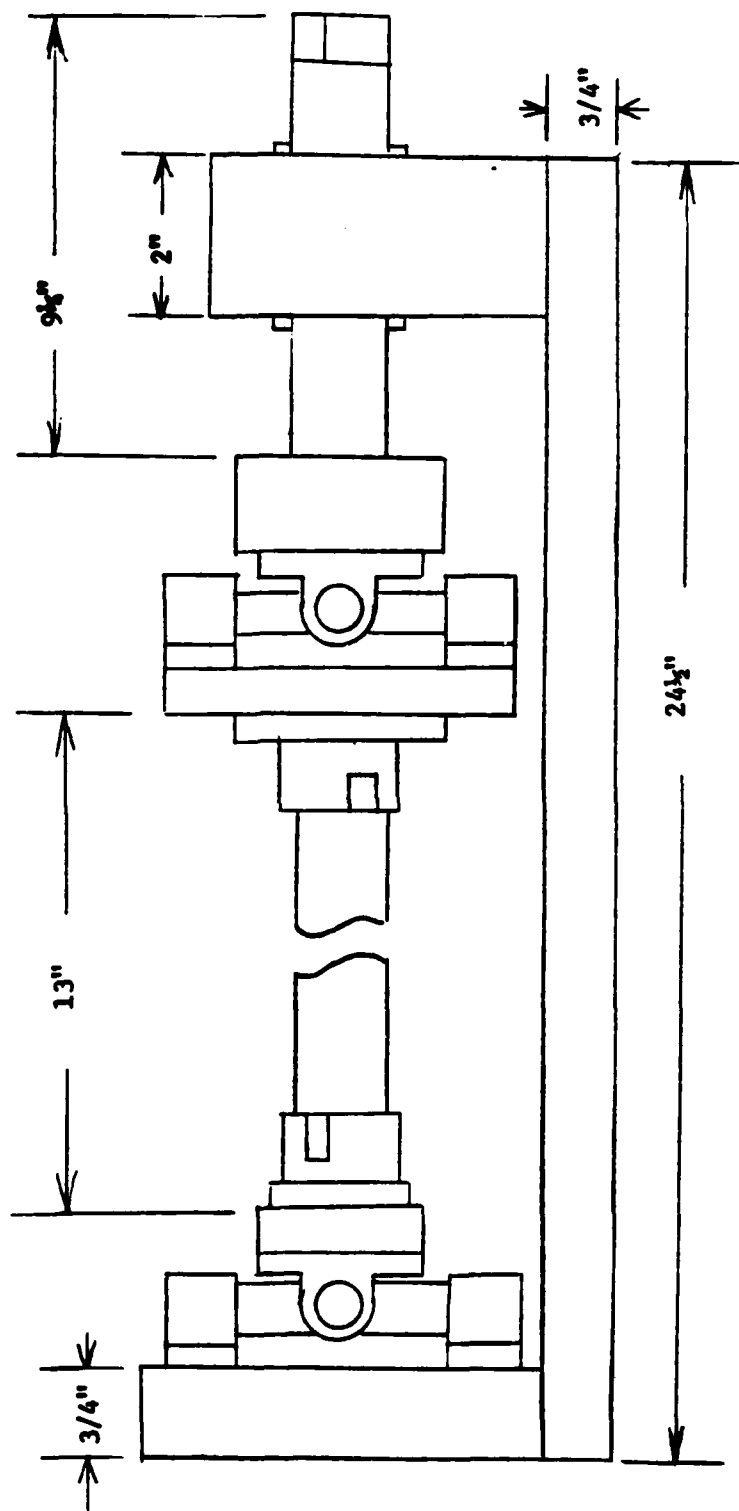
Figure 2.4 Torsion Testing Fixture—Dimensions

Brown and Sharpe
Stub Collet Holder and
1¼" collet

Lock and
Engaging Slot
(1/2 inch)

Specimen
End Cap

1 7/8"

1.030

1¼"
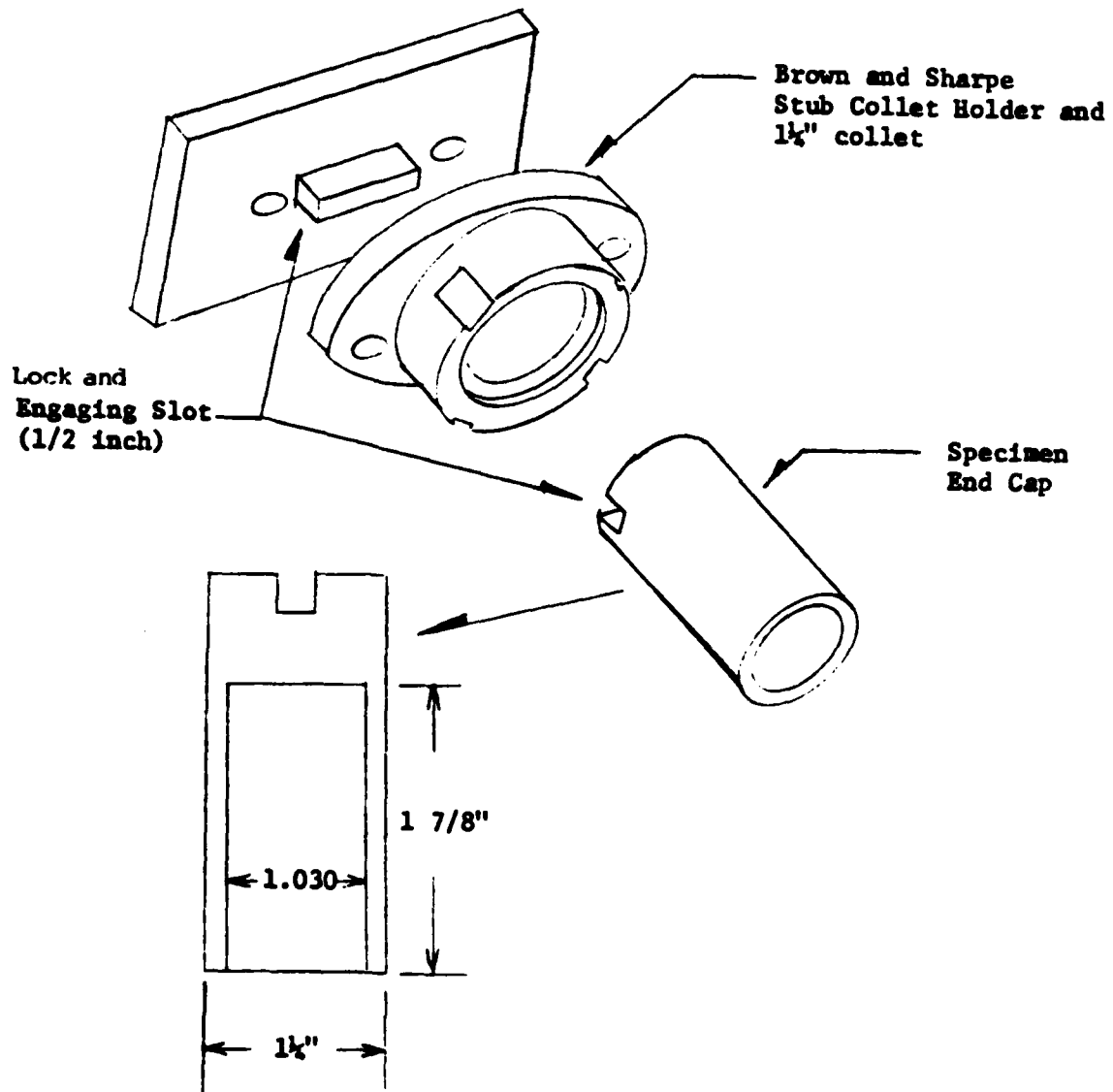
Figure 2.5 Detail of Torsion Specimen End Grips

as affected by transportation, or (2) by the lack of sufficient interference pressure during the curing process. The only available pressure during curing was obtained through the interfernece fit between the sleeve and alumina specimens largely due to thermal expansion of the adhesive.

The second adhesive tried was 3M Structural Epoxy, Scotch-Weld Brand, No. 2216 B/A. This gray two-part epoxy had less advertised strength, but it proved far more suitable even though a room temperature cure was used. Only in a very few cases did this adhesive fail. In all cases the epoxy was burned out after each test and a new specimen was bonded again. The burnout of end caps meant that fewer caps needed to be machined, thus, reducing expense considerably. The epoxy was also used to 'pot' the ceramic disks in place on copper gaskets in the disk tests as described in chapters 4 and 5.

The ceramic specimens used were made by McDanel Refractory of Beaver Falls. Pennsylvania. Their high density 988-Alumina and MV33-Mullite ceramic tubes were the specimens for both the bending tests of [1] and these torsion tests. The same materials and batches were also used for the disk tests of this report. For the disks. the method of casting was of necessity different. The tubes were extruded. Table 2.1 describes tube geometries.

	Alumina (998)	Mullite (MV33)
Mean and SD of Maximum OD	$1.0010 \pm .0021$	$1.0290 \pm .0065$
Mean and SD of Director 1 to Max. OD Direction	$.9985 \pm .0027$	$1.0236 \pm .0082$
Mean and SD of Minimum ID	$.6156 \pm .0203$	$.7276 \pm .0087$
Mean and SD of Direction 1 to Min. ID Direction	$.6209 \pm .0234$	$.7367 \pm .0074$
Estimated Outer Radius	.4999	.5132
Estimated Inner Radius	.3091	.3661
Test Length	7.3	7.3
Overall Length	11.0	11.0
Number of Samples Used for These Statistics	50	50

TABLE 2.1   TORSION SPECIMEN DIMENSIONS - INCHES

Chapter 3

RESULTS OF THE TORSION TESTS

Alumina 998 Results

Results for the torsion test of alumina are listed below in Table 3.1. It should be noted that most entries were considered successfully tested. Entries ranked 21 and 22 were used as 'good tests' even though they did not fracture; their epoxy bond failed first, but had a very high stress level. For that reason and because the high end of the curve might be more accurately depicted, it was decided to include them. Each of these other specimens actually fractured in torsion and their end caps were removed by heating the failed specimen end cap with an acetylene torch to burn out the adhesive. The cap was cleaned in a solvent. sandpapered. then reused. Thus. six sets of caps were required so that three were bonded to specimens being tested while three more were being cleaned on any work period. At two points. the mild. cold-rolled steel caps became deformed in the slot through plastic deformation so that new caps had to be manufactured. c.f., Fig. 2.5.

Table 3.2 lists all tests on alumina that were rejected. In the great majority of such tests the specimens slipped in the grips indicating bond failure. Two specimens that originally slipped at low levels were retested with new adhesive and were successfully tested to failure. Most tests in which bond failure occurred were never retested successfully. This is thought to be because those torsion specimens were found to be slightly undersized. thus. contributing to a thick bond of reduced sheer strength.

It was decided that any test which did not demonstrate failure through the specimen center would be rejected. This is because the most accurate representation of the Weibull Parameters was desired. Flaws near the attachments might propagate to failure by bond-induced stress concentrations, thus invalidation the results. No such examples occured: however. it

24

should be pointed out that most specimens exhibited a spiral shaped

crack through the grip attached to the torsion arm on the testing

machine - the active grip. This phenomenon was thought to result from

the release of strain energy in the heavy assembly through springback.

All such specimens failed in the gage - length end active grip.

The data were analyzed as a two-parameter Weibull distribution

through the use of an iterative programming code in Appendix I.

AUTO.FOR and AGARWA.FOR. The results for the alumina samples are

listed below:

Two-Parameter Family for Alumina 998

c = 0.617E-28 (in.^{2m} lbs.$^{-m}$):   2.708E-52 ($M^{2m} N^{-m}$)

m = 6.085 (dim less):   6.085 (dim less)

σ_u = 0 (psi):   0 (MPa)

σ_o = 4.325 E+4 (psi):   298.2 (MPa)

Residual error from curve fitting, Re = .3340E-01

where $Re = \sum_{i=1}^{N} W_i * (P_i - \tilde{P}_i)^2$

N = Number of entries

P_i = Probability of Fracture used as input

$\tilde{P}_i$ = Derived probability of Fracture. Table 3.3

W_i = Weight of each Data Entry.

Because probabilities of fracture vs. load, Table 3.1, were generated

by the rank method, the use of the three parameter distribution was not used.

Table 3 1. Torsion Experimental Results – Alumina 998
(Data from 24 good tests)

Specimen Number	Rank	Torque at Failure (Foot Pounds)	F(T̃) = 1/(N+1) (N=22)	Remarks
AT11	1	303.33	.0435	
AT62	2	373.75	.0870	
AT51	3	417.92	.1304	
AT20	4	429.74	.1739	
AT07	5	435.52	.2174	
AT21	6	460.83	.2609	
AT10	7	478.33	.3044	
AT06	8	517.92	.3478	
AT09	9	525.00	.3913	(Two specimens fractured at a load of 525)
AT12	(9)*	525.00	.3913	
AT25	10	530.83	.4348	
AT15	11	549.22	.4783	
AT61	12	552.50	.5217	
AT18	13	558.66	.5652	
AT60	14	575.00	.6087	
AT16	15	580.73	.6522	
AT64	16	585.00	.6957	
AT08	17	595.00	.7391	
AT56	18	600.00	.7826	
AT13	19	617.50	.8261	
AT14	20	659.17	.8696	
AT24	21	759.22**	.9130	Did not break -- adhesive failure
AT23	22	800.42**	.9565	Did not break -- adhesive failure

* Taken as same rank with twice normal weight

** These tests were included even though there was bond failure rather than
fracture because the load at failure was considerably above the mean of other tests.

Table 3.2. Data On All Other Alumina Tests

Specimen Number	Torgue at End of Test (Foot Founds)	Remarks
AT1	132.50	No end cap used -- initial set-up test.
AT2	100	Slipped in grip of initial design end slot.
AT3	100	Slipped in grip of initial design without end slot.
AT4	259.38	First modification of initial grip with no end slot but with roughened surface in contact with collet; it slipped.
AT5	259.38	First modification of initial grip with no end slot but with roughened surface in contact with collet; it slipped.
AT22	406.09	The following tests slipped in the bond with grip of latest design -- some were retested and still slipped. The specimens were discarded because they exhibited smaller than average outer diameters requiring a thick bond line; thus, making for a weakened test without machining undersized end caps.
AT53	200	
AT54	200	
AT55	200	
AT63	200	

The actual predicted fracture probability vs. load and input fracture probability vs. load, are given in Table 3.3 below. The probability of failure for a 1 inch^3 specimen is given by Graph 3.1 for equation parameters 3.1.

Specimen Rank	Probability of Fracture used as Input	Probability of Fracture from Equation 3.1	Weight
1	.04348	.01997	1
2	.08696	.06428	1
3	.13044	.13205	1
4	.17391	.15447	1
5	.21739	.16639	1
6	.26090	.22631	1
7	.30435	.27519	1
8	.34783	.40665	1
9	.39130	.43272	2
10	.43478	.45462	1
11	.47826	.52563	1
12	.52174	.53850	1
13	.56522	.56273	1
14	.60870	.62682	1
15	.65217	.64900	1
16	.69565	.66534	1
17	.73913	.70284	1
18	.78261	.72108	1
19	.82609	.78145	1
20	.86956	.89587	1
21	.91304	.99549	1
22	.95652	.99959	1

TABLE 3.3 Assumed and Determined Probabilities of Fracture for Alumina 998 Original Test Data
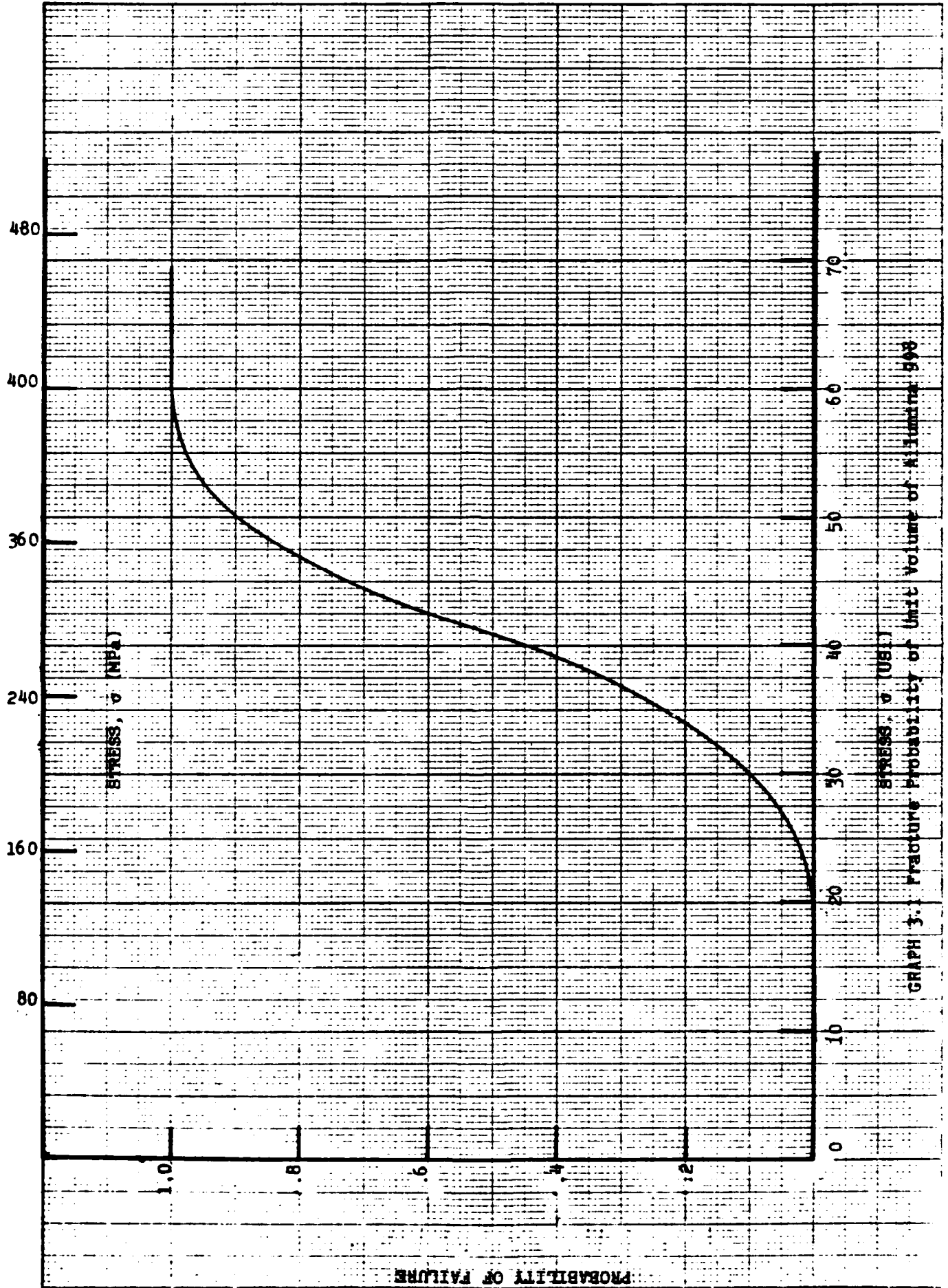
GRAPH 3.1 Fracture Probability of Unit Volume of Alumina 998

A photograph, Figure 3.1, demonstrates the fixture system immediately following one of the tests. Note the lack of crack propogation into the end-caps and the spiral nature of the fracture surface. Further examples of Alumina specimens just after failure depict samples AT60 and AT62. Attention again is drawn to the lack of any end cap fracture zone that was detectable. Again, a spiral fracture surface is evident that seems to initiate and terminate on a material bifurcation point or cusp persumably representing weakend material - Figures 3.2 and 3.3. Generally the Alumina tubes exhibited very high strengths in comparison to mullite. Some specimens did not fracture until surface tractions exceeded 50 ksi.

Mullite MV33 Results

Mullite Specimens selected randomly for the torsion test were labeled as depicted in Table 3.4. The Mullite (MV33) specimens exhibited somewhat less than $\frac{1}{2}$ the mean strength of the Alumina tubular specimens and were of a different mean dimension, Table 2.1. Because the Mullite was so much weaker, no end caps or adhesive bonds failed in these tests. For these specimens, the Weibull parameters were found to be:

$$c = .958E-27 \, (in^{2m} \, lbs^{-m}) \qquad 1.848E -51 \, (M^{2m} \, N^{-m})$$

$$m = 6.178 \, (dim'less) \qquad 6.178 \, (dim'less)$$

$$\sigma_u = 0 \, (psi) \qquad 0 \, (MPa)$$

$$\sigma_o = 2.3628E+4 \, (\sigma_o = c^{-1/m}) \, (psi): \quad 162.9 \, (MPa)$$

Residual Error from curve fitting = .3846E-01

As a measure of the fit of the derived distribution with the initial data, Table 3.5 provides a comparision. The graph 3.2 depicts the shape of the fracture curve for a 1 inch^3 volume subjected to uniaxial tension.

Figure 3-1. Torsion Test Device Immediately Following Test

Figure 3.2. Failed Alumina Torsion Specimen AT60

Figure 3.3. Failed Alumina Torsion Specimen AT62

Table 3.4. Torsion Experimental Results -- Mullite MV33
(Data from 24 good tests)

Specimen Number	Rank	Torque at Failure	$F(\tilde{T})=i/(N+1)$	Remarks
MT80	1	155.63	.0454	All mullite tests were success-
MT85	2	179.34	.0909	ful. None had to be duplicated
MT82	3	192.50	.1364	because the fracture loads were
MT90	4	211.46	.1818	significantly below those of the
MT84	5	247.71	.2273	alumina. Four specimens were
MT57	6*	250.00	.2727	inadvertently subjected to an oven
MT86	6*	250.00	.2727	cure by a research assistant who
MT79	7	256.67	.3182	thought the adhesive should be
MT83	8	258.33	.3636	baked. Those specimens were
MT72	9*	266.67	.4091	MT75, 76, 77, and 78. The data
MT73	9*	266.67	.4091	was used because the failure loads
MT81	10	274.48	.4545	appeared to be normal.
MT71	11*	276.25	.5000	
MT75	11*	276.25	.5000	Specimen 70 (MT70) was found to be
MT87	12	285.00	.5455	chipped and was discarded without
MT78	13	288.75	.5909	testing.
MT77	14	292.50	.6364	
MT59	15	292.88	.6818	
MT74	16	300.00	.7273	
MT76	17	300.83	.7727	
MT52	18	328.23	.8636	
MT88	19	339.17	.8636	
MT58	20	345.00	.9091	
MT89	21	360.00	.9545	

* Taken as the same rank with twice normal weight.

33
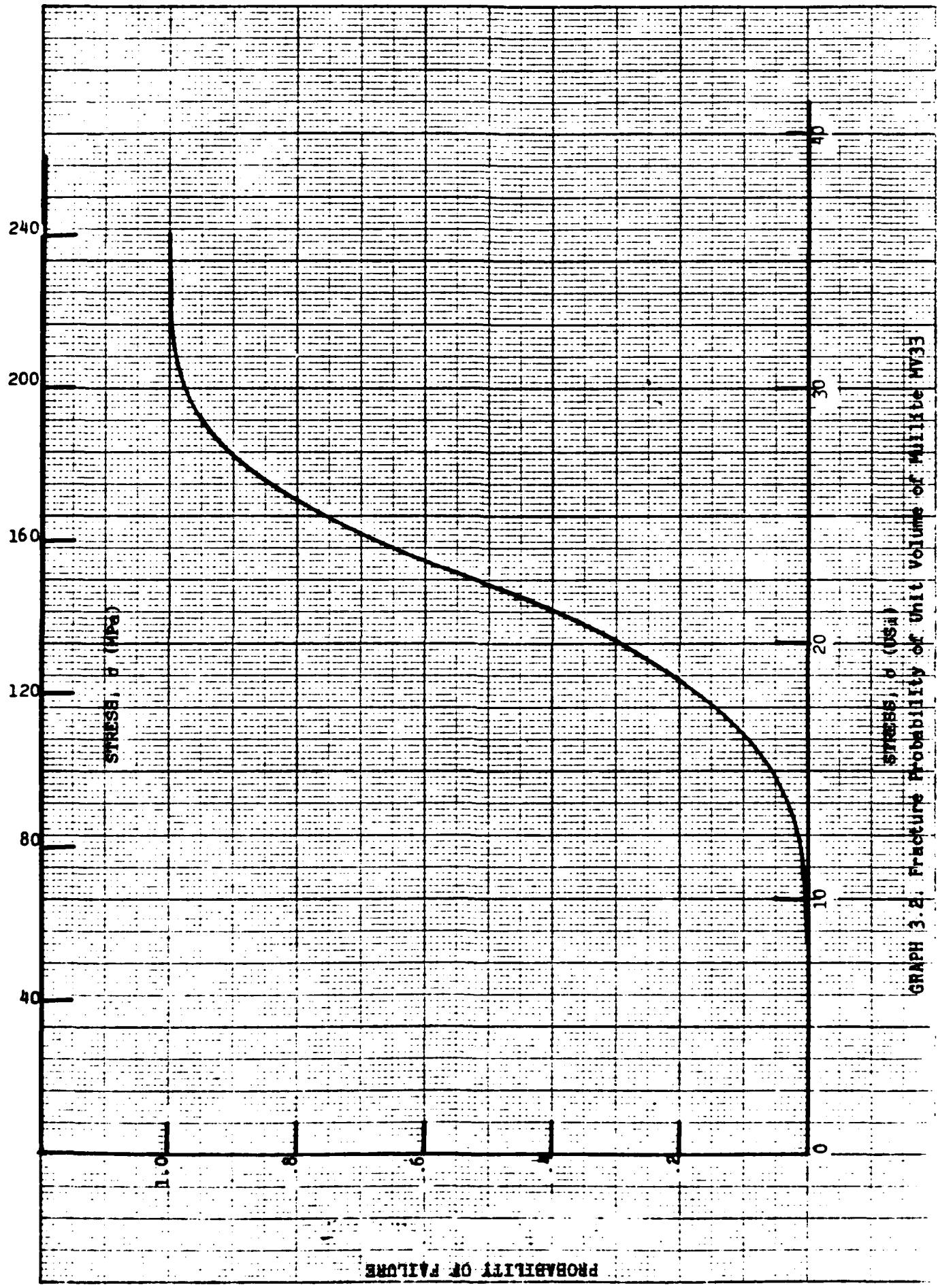
GRAPH 3.2. Fracture Probability of Unit Volume of Millikite HV33

Specimen Rank	Probability of Fracture used as input	Probability of Fracture from Equation 3.2	Weight
1	.04546	.01949	1
2	.09091	.04616	1
3	.13636	.07059	1
4	.18182	.12260	1
5	.22727	.29362	1
6	.27273	.30784	2
7	.31818	.35139	1
8	.36364	.36270	1
9	.40909	.42203	2
10	.45454	.40869	1
11	.50000	.49429	2
12	.54546	.56249	1
13	.59091	.59187	1
14	.63636	.62112	1
15	.68182	.62407	1
16	.72727	.67853	1
17	.77273	.68475	1
18	.81818	.86166	1
19	.86364	.91127	1
20	.90909	.93219	1
21	.95455	.96981	1

Table 3.5. Assumed and Determined Probabilities of Fracture for
Mullite MV33 Original test Data

The computer programs used to derive these data are interative
in nature which may seem inconsistent with the existence of a
closed form for the Weibull volume integral (1.3) and simple
Least Square solution available [1,3] for circular torsion specimens.
This approach, however, allows other minimization parameters to be
used as well as a 3-parameter model as appropriate.

It is interesting that the fracture of the mullite specimens differ substantially from the fracture of the alumina specimens. The difference, one of number and size of the fracture fragments, is similar to that observed in the bend tests although on a more dramatic scale. Figures 3.4, 3.5, 3.6, and 3.7 show that the fracture of mullite produces a great many more fragments than the alumina; the uniformity of the fracture patterns with generally a spiral geometry is unmistakable. This uniformity is thought to be a result of (1) the nearly constant strain energy density achieved in this type of test, and (2) the apparent lack of an appreciable stress concentration at the caps. Some of the specimens in the figures have failure well into the caps, Figure 3.4, through 3.7, and some do not, Figure 3.8.
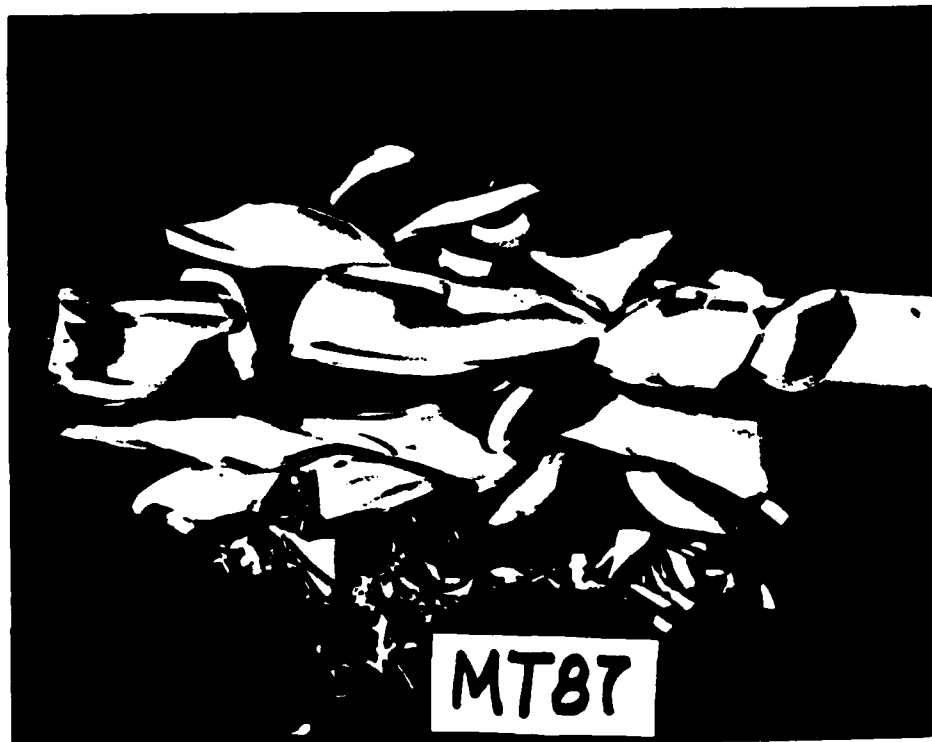
Figure 3.4. Mullite Failure in Torsion. Specimen MT87
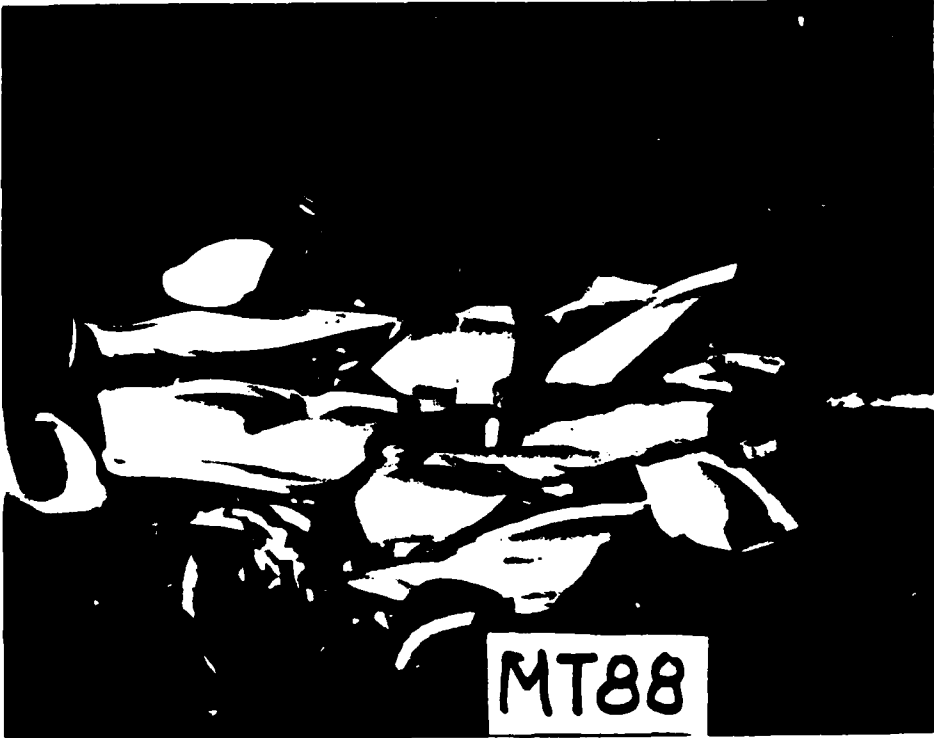
Figure 3.5. Mullite Failure in Torsion, Specimen MT88

Figure 3.6. Mullite Failure in Torsion, Specimen MT89

Figure 3.1. Mullite Failure in Torsion. Specimen MT90

The existence of specific bifurcation crack initiation points again
is in some evidence in the Mullite specimens. This material demonstrates
greater brittleness than Alumina, a finding also to be noted in the
pressure tests and in the 4-point loading tests of [1].

Chapter 4

Discription of the Hydraulic Test

The experimental designs and methods employed for the tube specimen
tests are characterized by nearly uniform stress states in the test section
except for the bending test where a constant principal stress ratio was
established. If there is symmetry of Weibull parameters as a function of the
direction, ϕ the angle between that point on the fracture surface and the
$\hat{n} = (1,1,1) \frac{1}{\sqrt{3}}$ direction, then the identification of these parameters at a
sufficient number of values of ϕ defines fracture. The table below describes
values of ϕ obtained by common tests.

ϕ Degrees	Test Type
54.7	Uniaxial tension or pure bending
39.2	Internal Pressure
90.0	Torsion
125.3	Compression

Table 4.1. Fracture Surface Angles for Typical Types of Tests

While neither compression nor internal pressure tests were conducted,
they could be employed on the same tube specimens. The test developed and
described in this chapter supplies a variety of stress ratios by hydraulically
loading disk specimens simply supported along their edges, Figure 4.1. This
test is necessary to complement fracture theory data gleaned from tube specimens
employing a single ϕ. Independence of the action of each principal direction
stress, a commonly applied assumption, can be evaluated in this way [4]. In
addition this hydraulic test may be an alternate to disk bend tests that
roughly approximate this method [5,6].
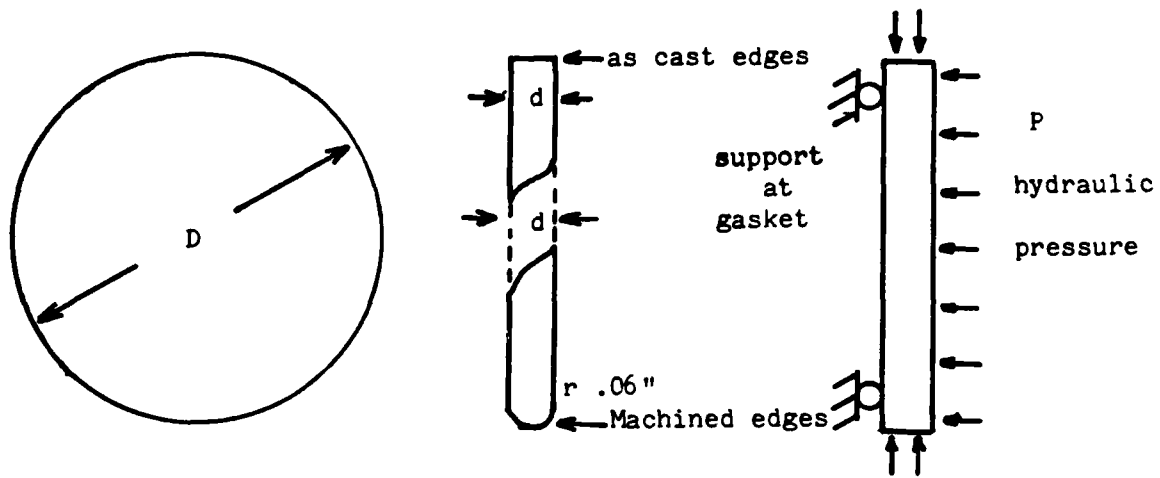
Figure 4.1.   Alumina and Mullite Disk Specimens and Loading Conditions

This also provides an additional geometry for application of Weibull theory. Both 'as-cast' samples and disks machined to ensure flat parallel surfaces were used as specimens in both Alumina and Mullite from the same batches as those of the tube specimens. D, d refer to the radius and thickness of 'as-cast' disks and D, d refer to those measurements of machined disks. The machined specimens were ground for flatness and for the removal of sharp edges, Fig 4.1. resulting in a radius of about .125". There was concern that 'as-cast' disks would be pre-disposed to warpage thereby causing considerable parasitic stresses during testing. In order to examine this potential problem, 'as-cast' and ground specimens in both alumina and mullite were all tested to failure. Their dimensions and deviations are given in Table 4.2 in reference to the geometries of Figure 4.1.

	D	d	d
Sample Type	Diameter (in)	Thickness at Center (in)	Thickness .25" From Edge (in)
Alumina - 'as-cast'	2.0210±.0140	.2522±.0038	.2519±.0034
Alumina - ground	2.0263±.0161	.2730±.0060	.2736±.0063
Mullite - 'as-cast'	2.0721±.0172	.2507±.0012	.2508±.0014
Mullite - ground	2.0533±.0196	.2488±.0058	.2502±.0048

Table 4.2 Disk Specimen Dimensions - means and standard deviations

In reference to Table 4.2, it apperars that the supplier selected thicker alumina samples for grinding and that grinding did not improve the overall thichness deviations.

While there have been numerous proposed disk specimens for brittle materials, the majority of such tests in checking Weibull parameters are of little value because either (1) they produce inordinately complex stress fields, (2) the mode of testing imparts high stress over a small volume, or (3) the small strain to failure requires the use of expensive high-precision samples and fixtures.

The test fixture of this report consists of a small hand-operated hydraulic pump capable of 10 ksi pressures and a pressure gage and tubing attached to the specimen testing assembly, Figure 4.2. In order to provide for simple support around the side of the specimen and to discourage leakage of hydraulic fluid, a soft copper gasket, cut to fit the assembly bolt pattern is bonded with 3M structural epoxy to the edge of the specimen, Figure 4.3.

The specimen with copper gasket is sandwiched between heavy steel members and held together by stiff preloaded bolts. One side of the specimen is in contact with pressurized hydraulic fluid while the other side is vented to the atmosphere through a 1-1/2 inch hole, Figure 4.4. The difference in a diameter of the specimen and vent provides a lip of 1/4 inch allowing contact with the soft copper seal to achieve a simply-supported condition. More detail is provided by Figures 4.5 through 4.7.

With each test the apparatus is disassembled through the removal of eight bolts and reassembled by the insertion of a new seal and bonded specimen. While some of the seals leaked perhaps due to plastic flow of the copper during the test, it is felt that a better seal design might alleviate this minor problem.

Before a new test is begun, the assembly is bled of air through a small valve; it is then placed in a safety cage. While this test does take longer to complete than the torsion or bending experiments of [1], it can be done in about five minutes by an experienced operator.
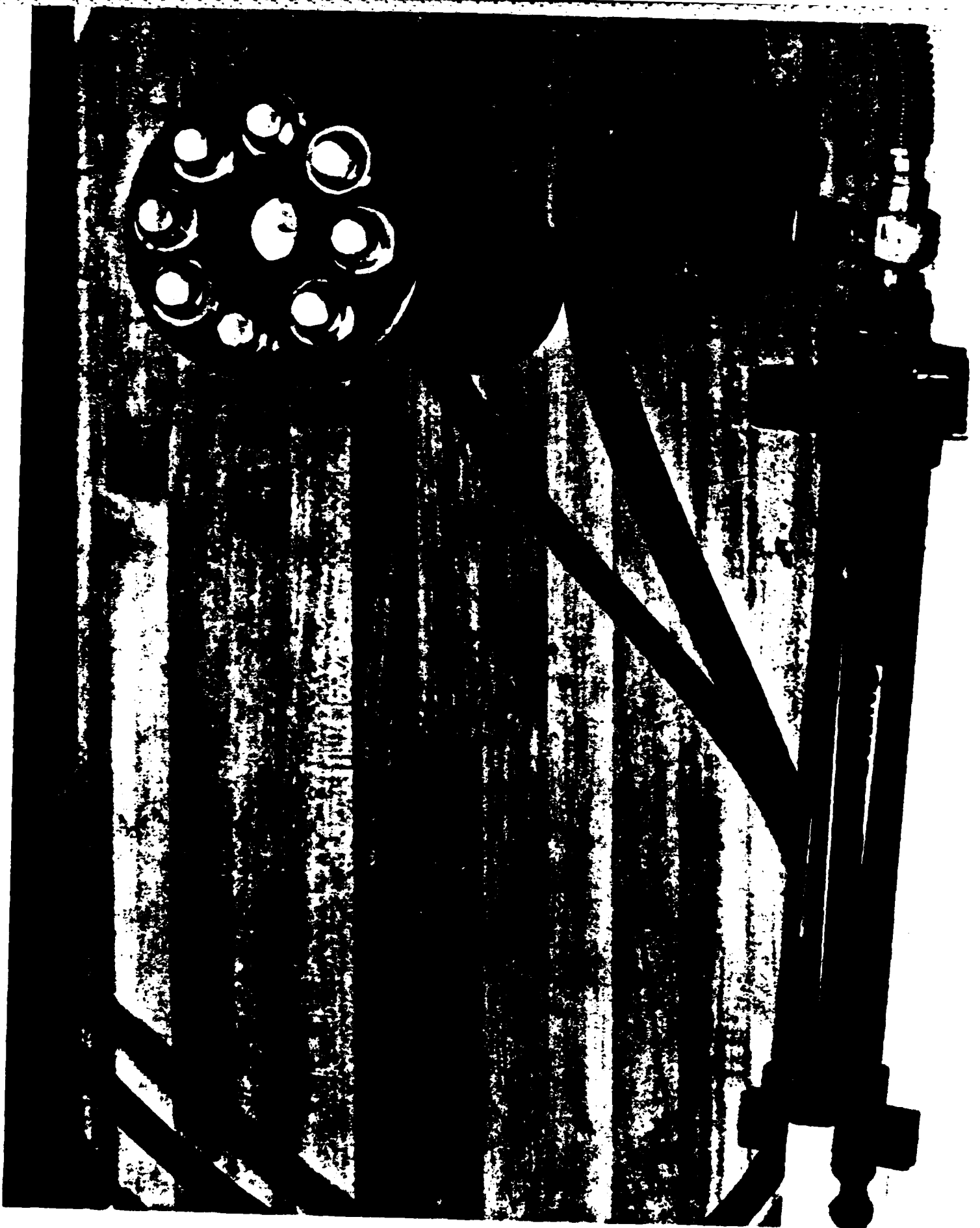
Figure 4-2. View of Hydraulic Test Assembly
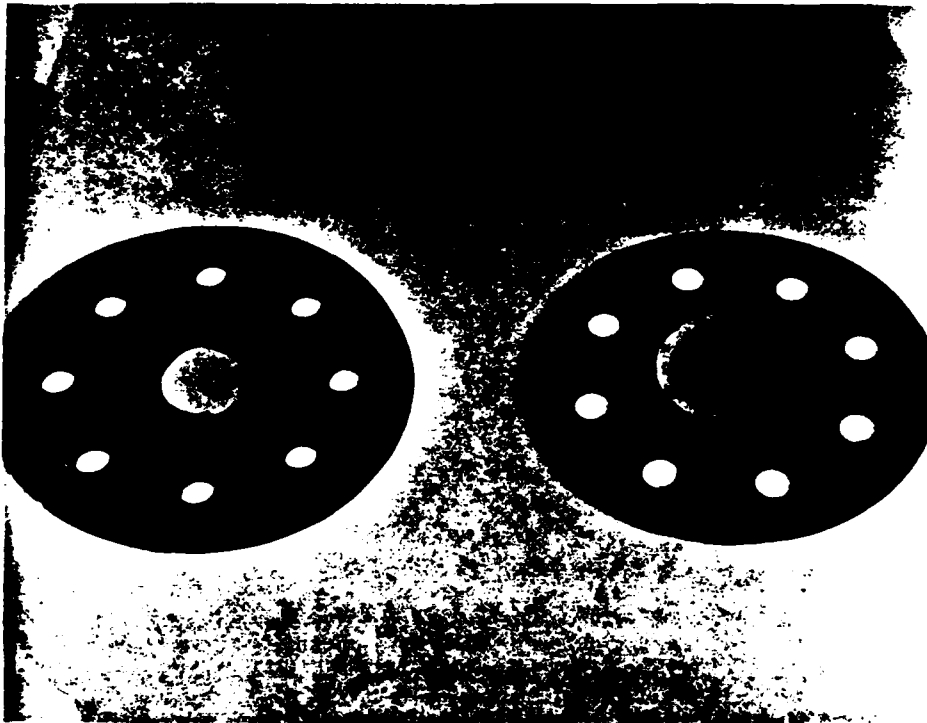
Figure 4.3. Specimen and Gasket – both sides
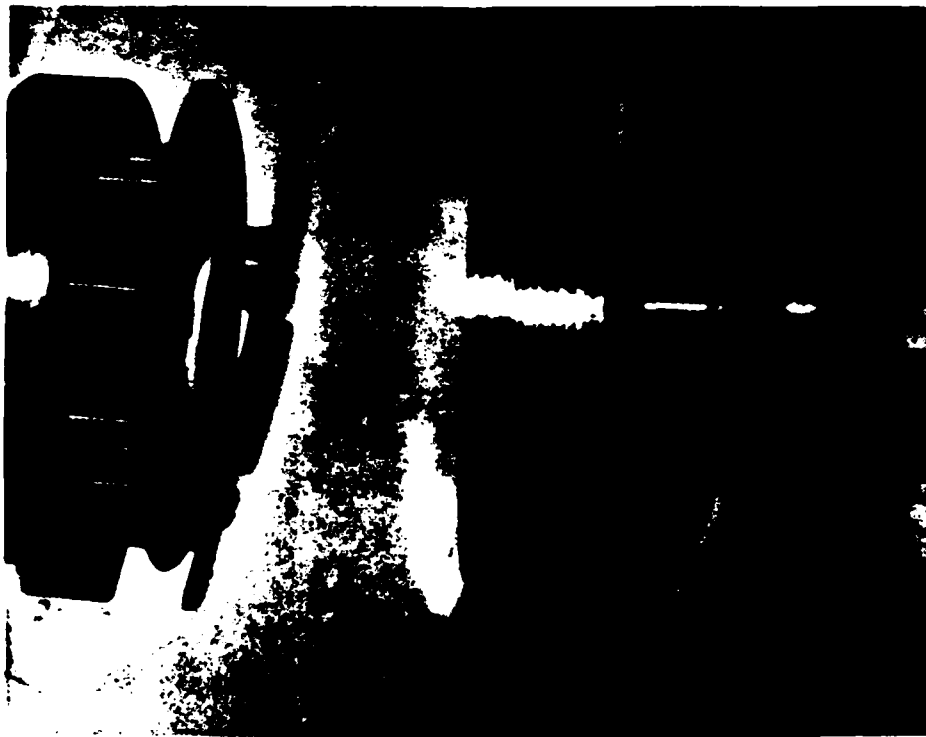
Figure 4.4. Specimen Ready to be Mounted in Assembly – Hydraulic Line and Vent to remove trapped air shown at right.

Fixture Made From SAE 4340–Ground Finish
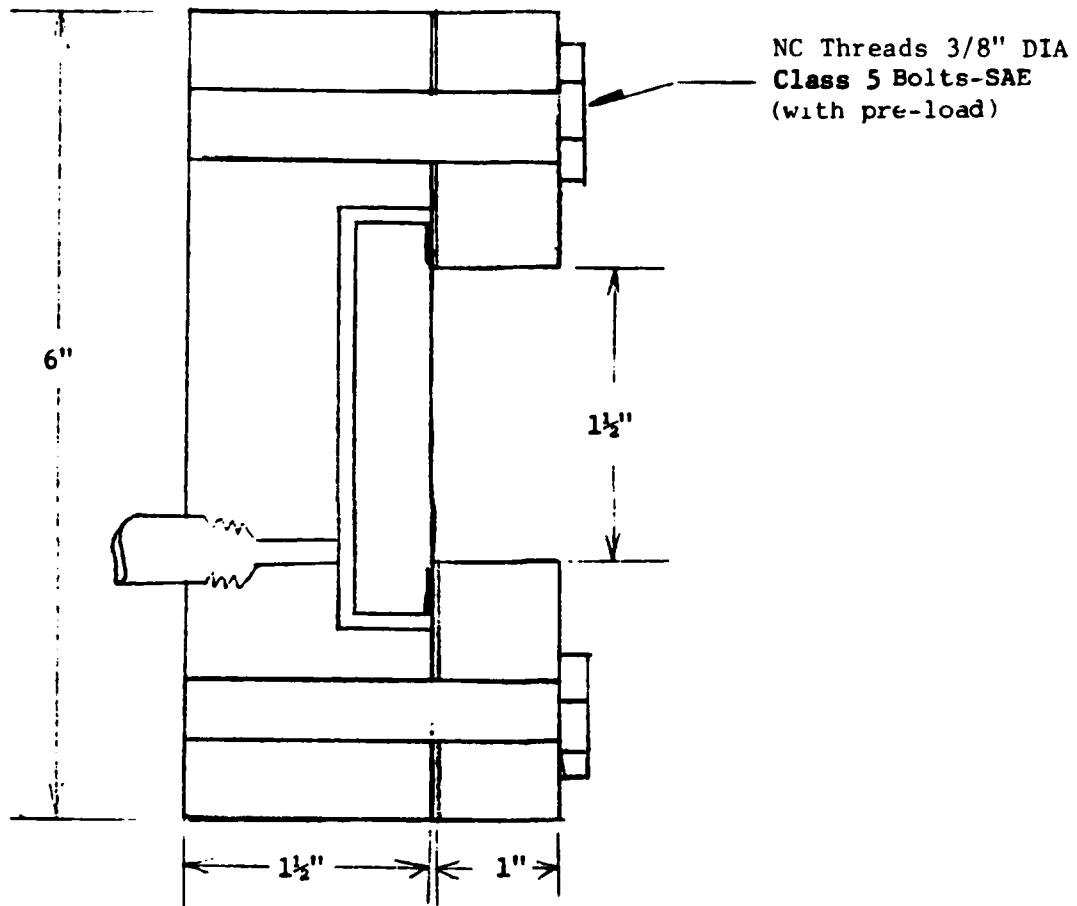
Figure 4.5. Disk Specimen Fixture

Valve and Coupling

Fixture Base

Specimen Gasket - 1/16" Annealed Copper

Fixture End Cap
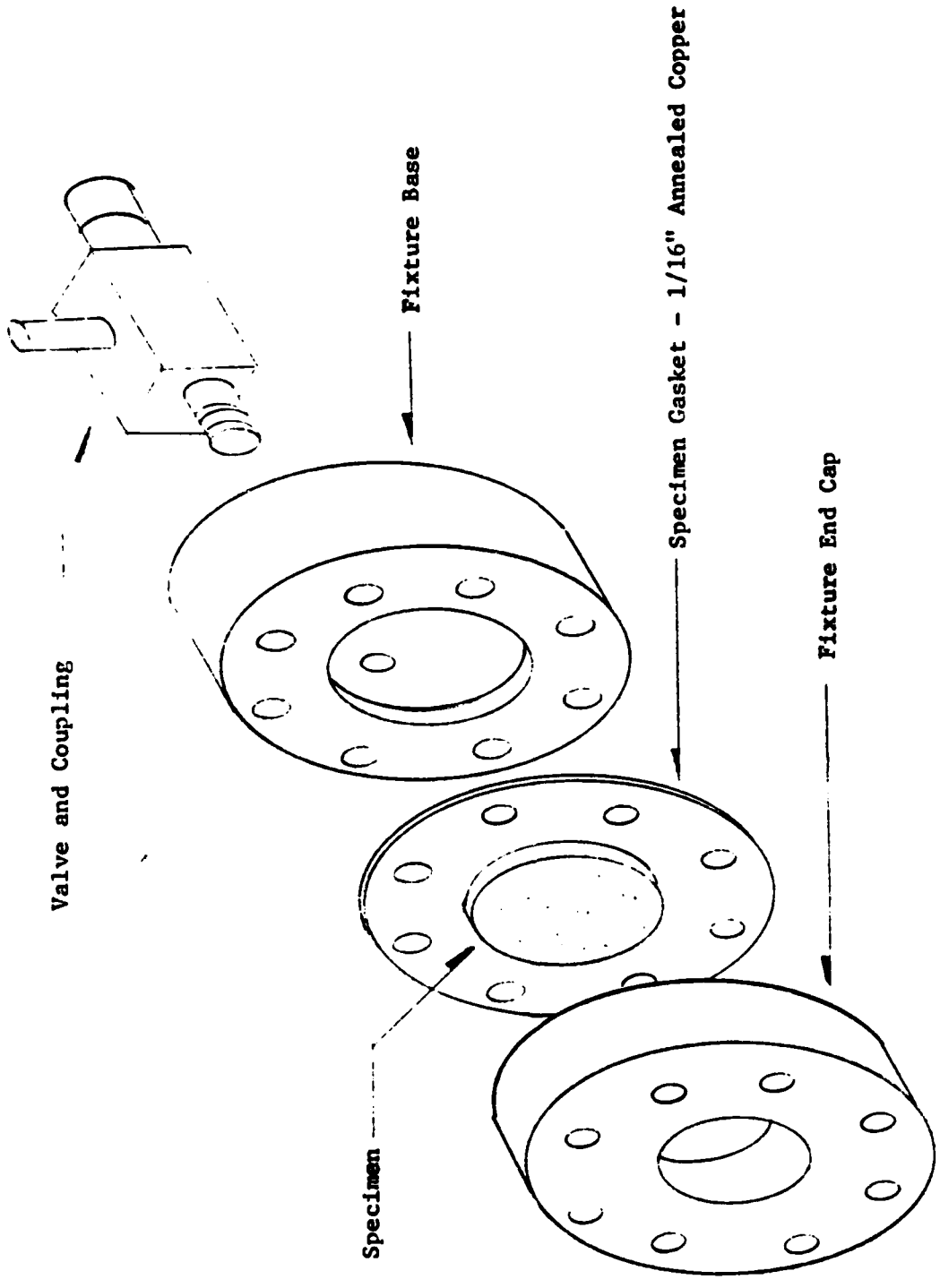
Specimen

Figure 4.6. Test Fixture for Disk Specimens

Test Fixture

Quick Connect Couplers

Valve and Flow
Direction Controller

Hose

Gauge
with non-return hand
for max pressure
record

Hand Pump

Gauge Adaptor
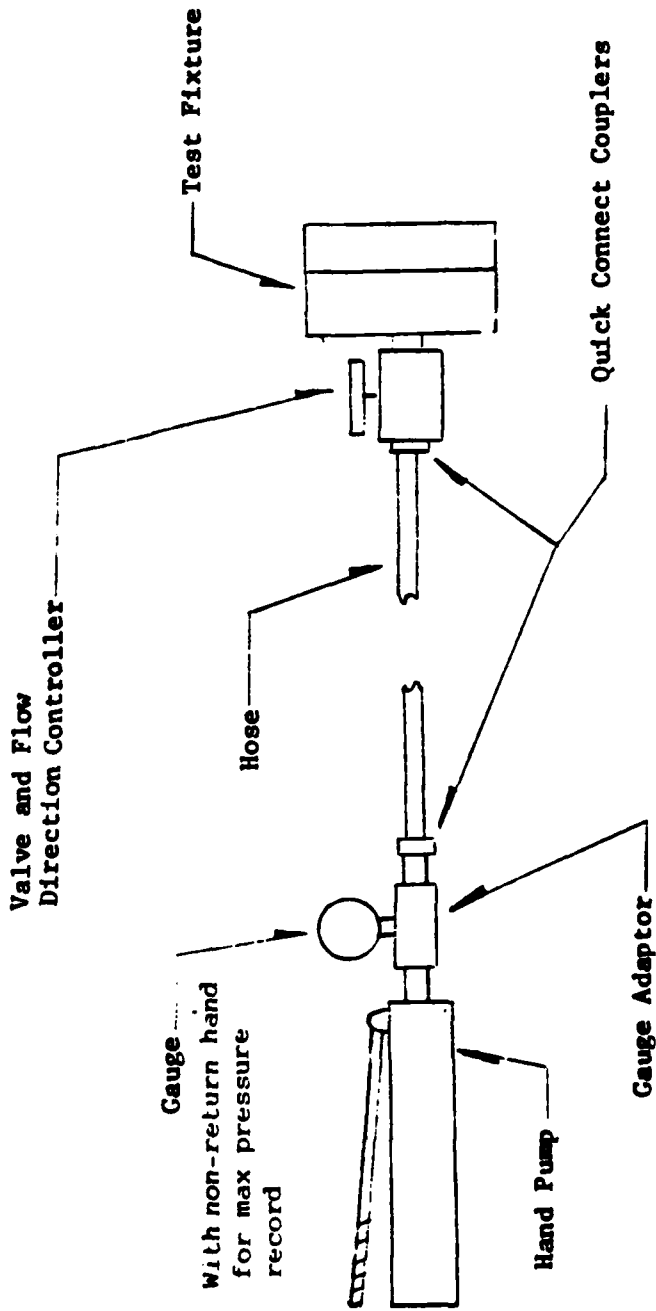
Figure 47. Schematic of Hydraulic System Capacity 10,000 p.s.i.

46

Following the Alumina tests, it was found that the apparatus could benefit from a device to help measure incipient specimen cracking. Particularly with alumina, the pressure at failure was not necessarily the pressure at which a crack first appeared. The alumina specimens seemed to arrest cracks growth until very high pressures were achieved. A conducting brittle coating over the outer side of the specimen with a balance bridge recorder might be of considerable benefit in detecting these initial cracks. Figure 4.8 depicts such devices.
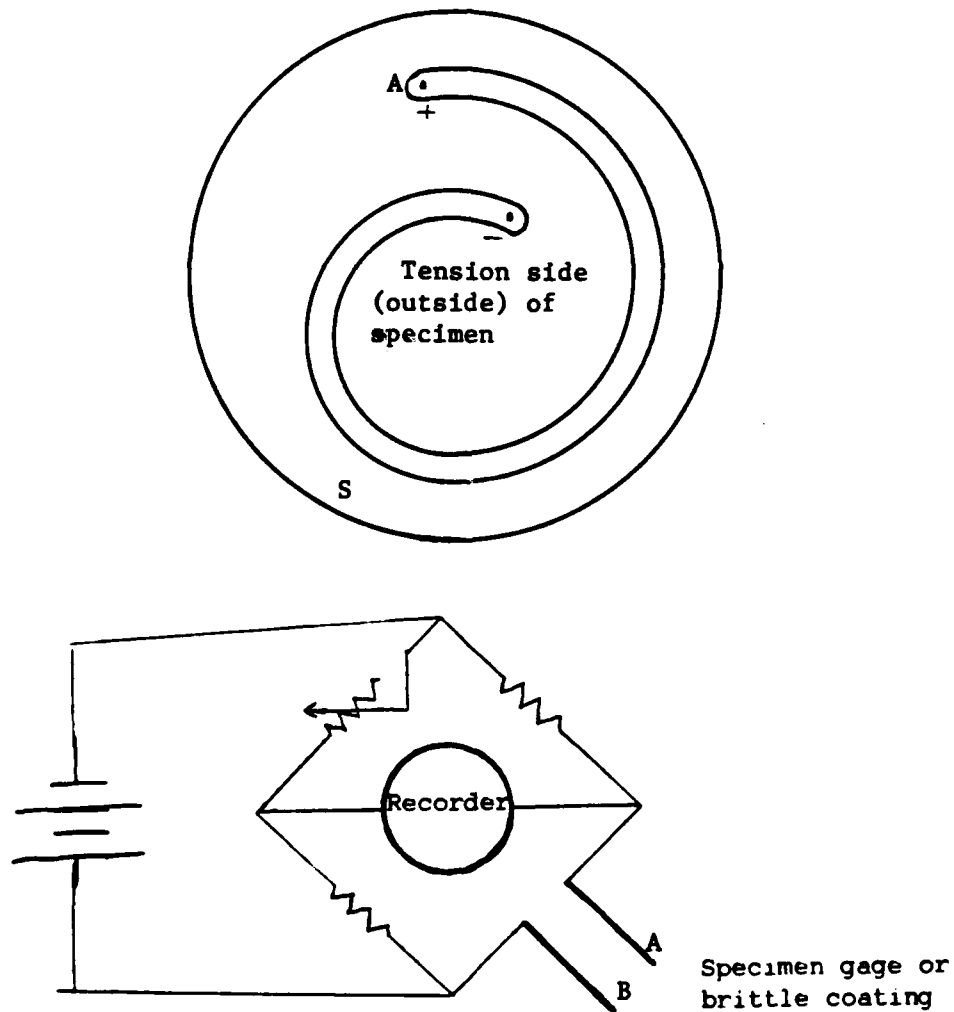
Figure 4.8. Specimens Coating Scheme and Bridge Crack Detector

47

Chapter 5

Results of the Hydraulic Tests

Both Alumina (998) and Mullite (MV33) disks made from the same batches as the tubular specimens of [1] were tested to failure through hydraulic pressure applied to one surface. The experiment was designed to approximate simple support at the outside where the soft copper seal was compressed between the specimen and pressure retainer.

Actual test results performed on alumina are ranked for (as-cast) disks, Table 5.1a, and for ground-finish disks, Table 5.2a. Four of these specimens in each group, Table 5.1b and 5.2b, could not be fractured due to leaky seals.

The mean strength for ground specimens over 'as-cast' specimens (alumina) showed about a 16.2% increase based on a total of 21 successful as-cast, and 17 successful ground-finish disks.

The leaky seals encountered in both sets of alumina specimen tests all occured at nearly no pressure reading. Thus, they were not the result of normal gasket failure in the copper but rather a result of potting material failure in the epoxy which was employed in a highly unusual fashion. Because equal numbers of as-cast and ground finish samples could not be tested due to leaks, this phenomenon is was thought not to be related to specimen warpage.

Of further concern in establishing table 5.1a and 5.2a is the fact that the actual pressure level at which fracture occured in the alumina specimens was difficult to determine with precision. Typically specimens failed without an apparent noise or an abrupt pressure drop. Rather, the alumina samples began to ooze hydraulic fluid as the operator attempted to sustain or increase pressure levels. The figures cited in Tables 5.1a and

Table 5.1a. Alumina Disk (as cast) Pressure Tests
(Mean Pressure at Failure = 2860 p.s.i.)

Specimen Number	Applied Pressure at Failure (p.s.i.)	Remarks
		All tests were normal
A24P	1400	
A25P	1500	
A22P	2000	
A10P	2175	
A13P	2225	
A14P	2350	
A12P	2400	
A1P	2550	
A17P	2750	
A16P	2925	
A23P	2970	
A26P	3000	
A29P	3050	
A0P	3200	
A1P	3200	
A11P	3350	
A28P	3400	
A15P	2500	
A27P	3670	
A18P	3950	
A30P	4500	

Table 5.1b. Alumina Disk (as cast) Pressure Tests
The following specimens were rejected.

Specimen Number	Maximum Applied Pressure	Remarks
A3P	Not recorded	Leakage at seal
A4P	Not recorded	Leakage at seal
A5P	Not recorded	Leakage at seal
A6P	Not recorded	Leakage at seal

Table 5.2a. Alumina Disk (ground finish) Pressure Tests
(Mean Pressure at Failure = 3365 p.s.i.)

Specimen Number	Applied Pressure at Failure	Remarks
A31P	2360	All test were normal
A41P	2635	
A45P	2750	
A35P	2790	
A8P	2800	
A7P	2900	
A9P	2955	
A42P	3000	
A20P	3150	
A38P	3150	
A33P	3190	
A19P	3650	
A39P	3695	
A32P	3985	
A40P	4500	
A44P	4600	
A21P	5100	

Table 5.2b. Alumina Disk (ground finish) Pressure Tests

The following specimens were rejected.

Specimen Number	Maximum Applied Pressure	Remarks
A34P	Not recorded	Leakage at seal
A36P	Not recorded	Leakage at seal
A37P	Not recorded	Leakage at seal
A43P	3400 p.s.i.	Produced fracture to one side

5.2a essentially represent a pressure at which significant sustained leakage occured through an identifiable crack. It generally could not be exceeded through the use of a hand operated ram.

The test results for Mullite are given for as-cast samples in Table 5.3a and for ground samples in Table 5.4. The average strength was considerable below that of alumina which may have accounted for fewer failures due to leakage. The as-cast seal failures are given in Table 5.3b. There were no failures in the mullite ground finish specimens. With the mullite disk test there is a 10% difference between average strengths of as-cast tests over ground test, a trend that is opposite that of the alumina disks. A further variance of the mullite results is that three samples in the Table 5.3b failed via a single diagonal crack. These are not included in Table 5.3a due to the concern that wrapage of the as-cast specimens may have produced these anomalies.

A further difference in the testing of Alumina and Mullite disks is that when mullite disks fail, there is an instantaneous pressure drop and an unmistable crack in the specimen. In addition to the tabulated results of the pressure test, there is additional information to be gleaned from an observation of the fractured specimens. In the photo reproductions that follow, it is important to note that each specimen is labeled with or without a trailing "P" in the specimen number. All disk specimens in Tables 5.1 - 5.3 have a "P" suffix to avoid confusion with tube specimens. This "P" indicates the specimen side exposed to hydraulic fluid pressure and the specimen number with no "P" indicates the external or atmospheric side. Thus, for hydraulic specimen, A13P, a photograph of its sides will be labeled A13 (outside) and A13P (inside). The outside surface photos can also be detected by the adhesive that protrudes at the edge.

Table 5.3a. Mullite Disk (as Cast) Pressure Tests
(Mean Pressure at Failure = 1814 p.s.i.)

Specimen Number	Applied Presure at Failure	Remarks
M120P	1000	
M114P	1100	
M119P	1100	
M117P	1200	
M121P	1210	
M122P	1290	
M123P	1300	
M126P	1300	
M109P	1450	
M125P	1450	
M101P	1500	
M115P	1500	
M110P	1750	
M108P	1850	
M103P	1900	
M116P	2100	
M113P	2400	
M124P	2450	
M99P	2650	
M100P	3700	
M102P	3900	

Table 5.3b. Mullite Disk (as Cast) Pressure Tests
The following specimens were rejected.

Specimen Number	Maximum Applied Pressure	Remarks
M104P	950	Single, large, diagonal break
M105P	900	Single, large, diagonal break
M106P	800	Single, large, diagonal break
M107P	Not Recorded	Leak at seal
M111P	Not Recorded	Leak at seal
M112P	Not Recorded	Leak at seal
M118P	Not Recorded	Leak at seal

Table 5.4. Mullite Disk (Ground Finish) Pressure Tests
(Mean Pressure at Failure = 1638 p.s.i.)

Specimen Number	Applied Pressure at Failure	Remarks
M202P	600	
M201P	1280	
M200P	1410	
M205P	1430	
M207P	1525	
M208P	1750	
M203P	1900	
M204P	2200	
M206P	2650	

A series of two alumina photos are listed for both specimens A11P and A13P. Figure 5.1a shows the outer side and 5.1b shows the inside. The inside of this specimen and of others are shown in greater magnification to provide enhanced evidence of cracks. It is interesting that this specimen gives no indication of a crack on its compression or inner surface although there is a radial or 'crow foot' pattern in the outer surface, Figure 5.1a. This type of crack was typical of almost all alumina specimens such as Figure 5.2a (outside) and 5.2b (inside). While the outside surface exhibited a series of hairline width cracks, no visual crack could be detected on the inside. Indeed there was little change in pumping pressure as detected by the test operator. In fact, with the alumina, pressures could be re-elevated provided the pumping rate exceeded the small leakage rate through the specimen. There was an attempt to detect incipient cracking by listening while observing the specimens by closed circuit TV. In the case of alumina, this revealed nothing.

Several of the alumina specimens were later cleaned; they appeared still to be intact except for the hairline cracks made visible by rubbing the surface with graphite mixture. Again, future tests could benefit from an addition of a conducting brittle strip to aid in crack detection. These specimens appeared to have cracks, Figures 5.1 and 5.2, that propagated to depth of about 50 mm to 70 mm under the outer surface where they appeared to arrest. The exact cause of the hydraulic leak in alumina seems to have been due to seepage through internal cracks that became sealed after the test and not by leakage at the seal.

The corresponding tests on mullite showed a great deal of difference in both the strength of the specimen and in the fact that again fracture appeared much more definite and catastrophic. In specimen M108, representative of mullite samples, fracture is through the entire thickness of

54

the specimen, Figure 5.3a (outside surface) and Figure 5.3b (inside surface). While the fracture is through the entire thickness, the pattern on the two surfaces is greatly different indicating that the crack has not propagated uniformly throughout the mullite. There is considerable evidence of spalling on the pressure (compression) side of this specimen while a lesser amount of material has been lost at the outer side.

Specimen M115 shown in Figures 5.4a and 5.4b provides a more complex fracture pattern although no spalling can be noted. Again, it is seen that the surface crack patterns are greatly different on the inside and outside. In about all cases the radial ray or 'crow foot' fracture pattern was noted. This was observed in both alumina and mullite failed samples and is thought to be the result of a similar stress field with radial symmetry with failure occuring along rays where the material is statistically weak.

Figure 5.1a. Hydraulic Fracture Specimen A11 – Outer Surface (2.5X)

Figure 5.1b. Hydraulic Fracture Specimen A11P – Inner Surface (3X)
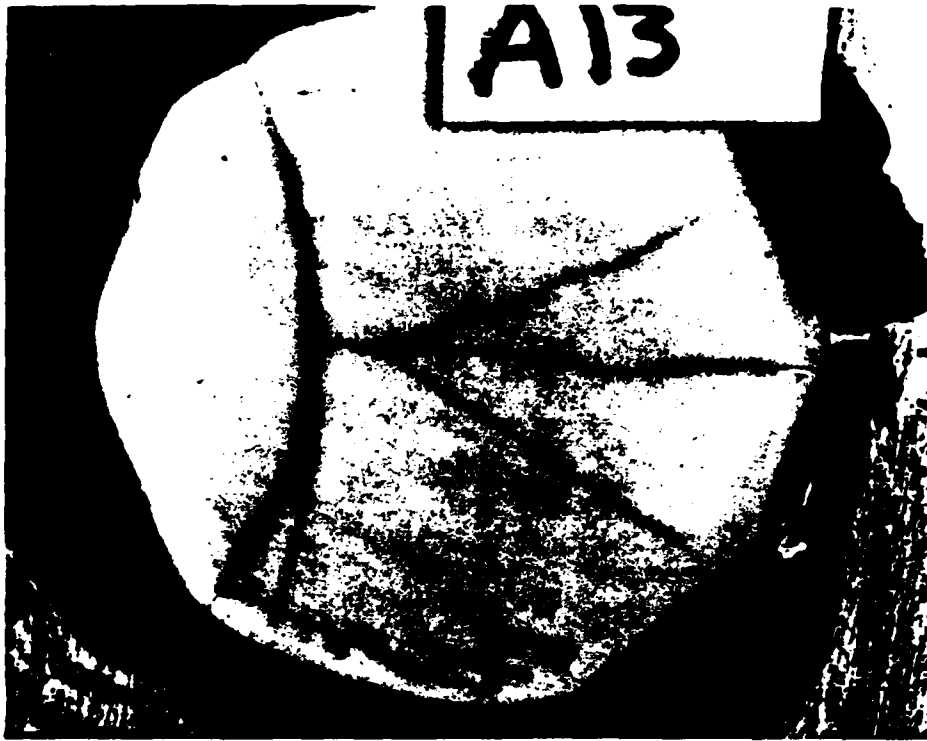
Figure 5.2a. Hydraulic Fracture of Specimens A13 –
Outer Surface (2.5X)

Figure 5.2b. Hydraulic Fracture of Specimens A13P –
Inner Surface (3X)
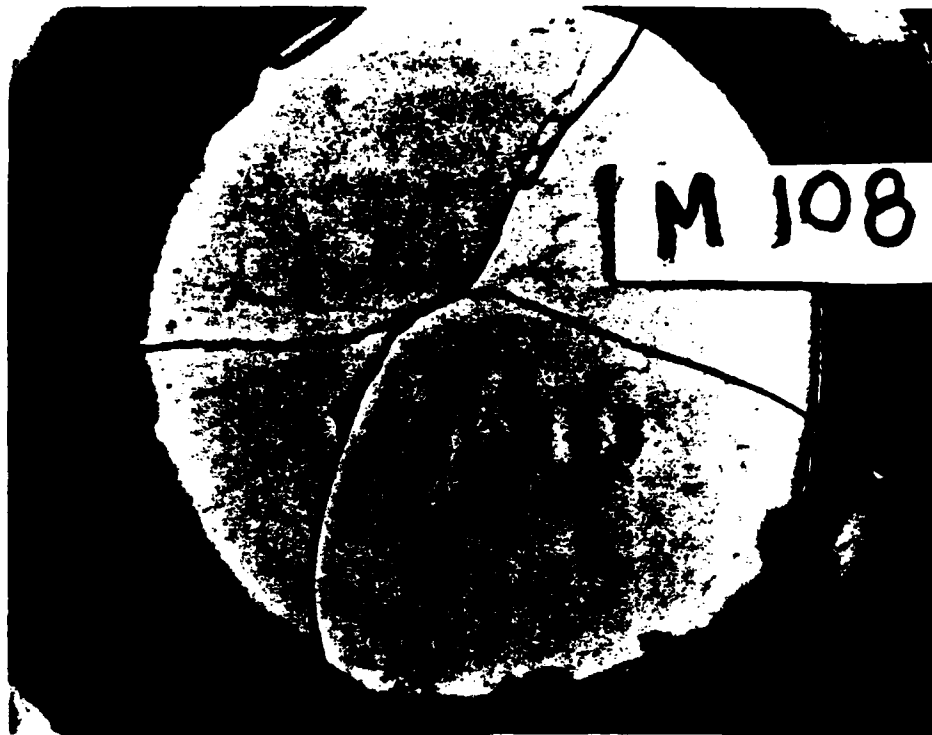
Figure 5.3a. Hydraulic Fracture of Specimen M108 –
Outer Surface (2.5X)
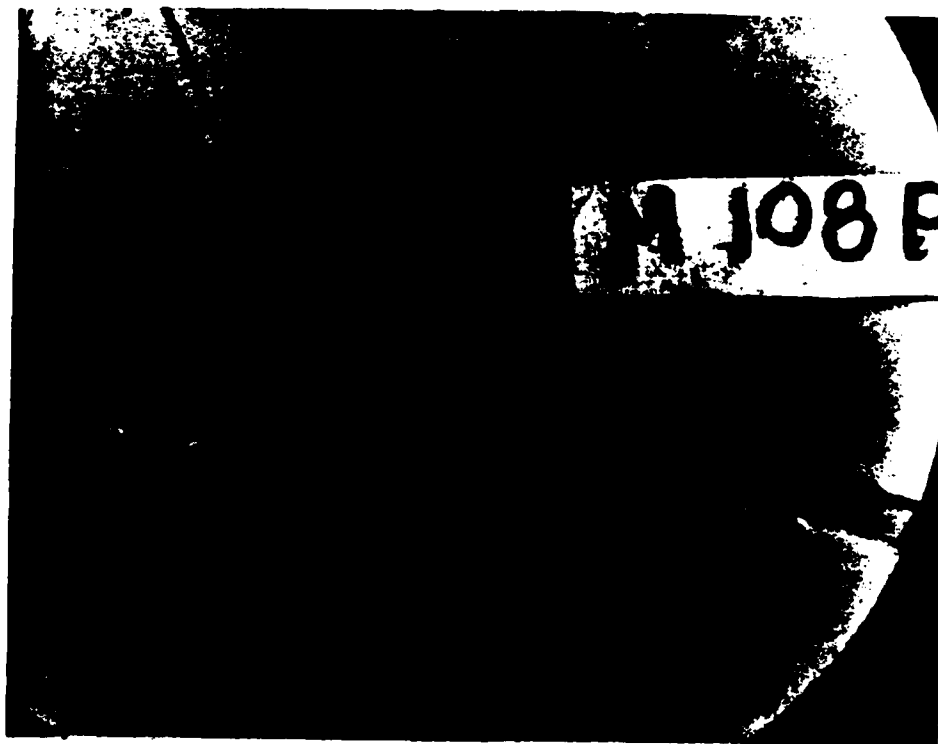
Figure 5.3b. Hydraulic Fracture of Specimen M108P –
Inner Surface (3X)
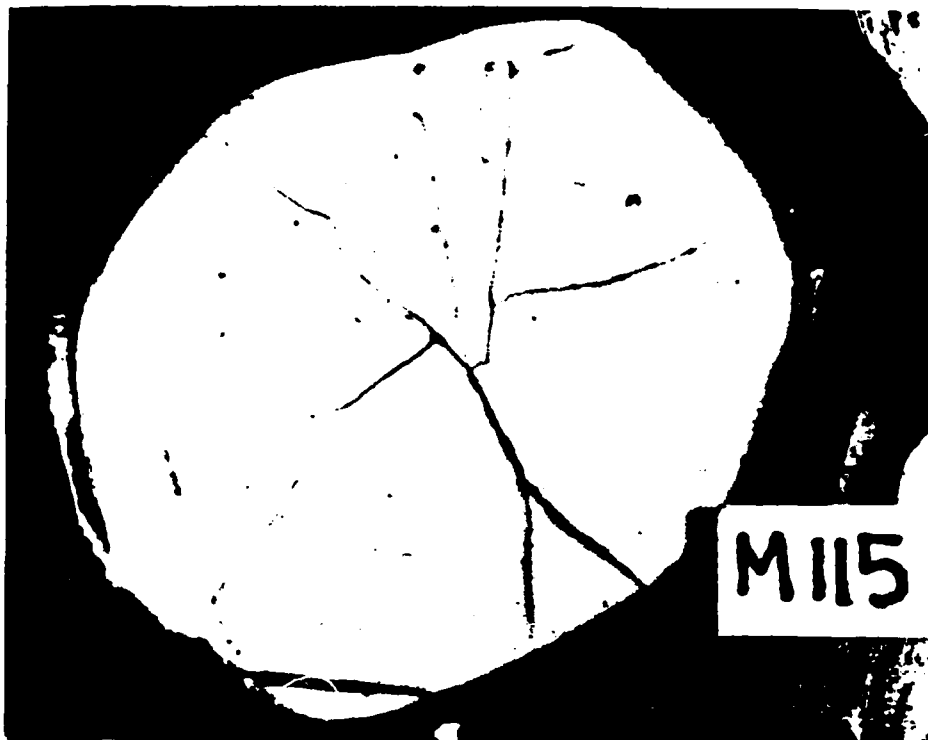
Figure 5.4a. Hydraulic Fracture of Specimen M115 -
Outer Surface (2.5X)

Figure 5.4b. Hydraulic Fracture of Specimen M115P -
Inner Surface (3X)

Chapter 6

Conclusion

The experimental investigations embodied by Navair Reports N00019-78-C-0520 and N00019-79-C-0574 form a set of experiments that provide Weibull data on bending and torsion for tube specimens and for a uniformly loaded circular plate. General conclusions are:

1) The feasibility of torsion and bending tests on one specimen geometry of a class of ceramic material has been demonstrated. Evidence of erratic results produced by stress concentrations near points of load application is not significant.

2) The use of inexpensive tube geometries may reduce the cost of ceramic specimen tests when complemented by the experiments, theory and programming techniques of this report.

3) The use of hydraulic pressure in providing a suitable loading mechanism has been demonstrated. Improvements to this technique may however be:

  a) the use of a simple retaining bladder to restrict hydraulic fluid excursion and seepage into potentially porous specimens.

  b) the inclusion of a fracture detecting brittle conductive coating or other techniques to provide a more precise measurement of incipient fracture in materials that have some fracutre arresting capability such as the alumina tested.

  c) the modification of current copper seals and specimen bonding materials or techniques to reduce reject tests.

4) A thorough analysis is yet to be made of the disks to test whether or not raw Weibull data can accurately predict failure distributions in materials to which a complex stress field is applied. Such a study is ongoing and will be the subject of a forthcoming submitted publication.

REFERENCES

[1] Craft, W. J., and Filatovs, J. G., "Fracture Prediction on Brittle Materials," Naval Air Systems Command Final Report N00019-78-C-0520, May 29, 1981.

[2] Hoffman, Oscar, and Sachs, George, Introduction to the Theory of Plasticity for Engineers, McGraw Hill, 1953.

[3] Weil, N. W., and Daniel, I. M., "Analysis of Fracture Probabilities in Non-Uniformly Stressed Brittle Materials," American Ceramic Society Journal, Volume 47, No. 6, June 1964.

[4] Barnett, R. C., et al., " Utilization of Refractory Non-Metallic Materials in Future Aerospace Vehicles," Flight Dynamic Laboratory, Air Force Systems Command, Contract No. AF33-(615)-1494, Sept., 1965.

[5] Shetty, D. K., Rosenfield, A. R., Bansal, G. K., and Duckworth, W. H., "Biaxial Fracture Studies of a Glass-Ceramic," Journal of the American Ceramic Society, Volume 64, No. 1, January 1981.

[6] Marshall, David B., "An Improved Biaxial Flexure Test for Ceramics," Ceramic Bulletin, Volume 59, No. 5, 1980.

```fortran
        PROGRAM TORSIO
C THIS PROGRAM GIVES WEIBULL PARAMETERS FOR TORSION
        REAL L
        DIMENSION EPF(40),W(40),AA(3), P(40)
        DIMENSION VAR(3,3),RES(3,3)
        COMMON/PAR/K,L,C,T(40),EJ,SIGU,EM,RO,RI,TPF(40)
        WRITE(5,40)
40      FORMAT(2X,'ENTER DATA FILE NUMBER AND ITER FRPOP ROUND')
C K=NO OF DATA POINTS
C T=TORQUE AT RUPTURE
        READ(5,*) ND,ERP
        READ(ND,*) K
        DO 400 I=1,K
        READ(ND,*) T(I),W(I)
        T(I)=12.*T(I)
C THIS IS TO CONVERT FROM FT.LB. TO IN.LB.
C THE FILE'S UNITS ARE FT.LB.
400     CONTINUE
        X=FLOAT(K+1)
C NOW RANK THE DISTRIBUTION
        DO 1 I=1,K
1       EPF(I)=FLOAT(I)/X
        READ(ND,*) L,RO,RI
        EJ=3.1416/2.*(RO**4-RI**4)
C L=GAGE LENGTH OF SPECIMEN
C RO=OUTER RADIUS OF SPECIMEN
C RI=INNER RADIUS OF SPECIMEN
C EJ=POLAR MOMENT OF SPECIMEN
        WRITE(5,59) L,RO,RI,EJ
59      FORMAT(/,2X,'L=',1X,F8.4,' RO=',1X,F8.4,' RI=',1X,F8.4,
     1  ' EJ=',1X,E10.5)
        GO TO 11
111     WRITE(5,112) C,EM,SIGU,RES(1,3)
112     FORMAT(1X,'C,EM,SIGU,RESE',4E15.6)
11      WRITE(5,42)
42      FORMAT(1X,'INPUT EM,SIGU, AND ICODE FOR C ITERATION')
        READ(5,*) EM,SIGU,ICODE
        IF (ICODE.EQ.1) GO TO 90
        SIGMAX=T(K)*RO/EJ
        DEN1=(SIGMAX-SIGU)**EM
        ENC=ALOG(2.)/DEN1
        VAR(1,3)=ALOG(2.*FLOAT(K))/DEN1
        CN=0
C NOW BEGIN C ITERATION TO MINIMISE RES
        WRITE(5,69) VAR(1,3),ENC
69      FORMAT(1X,'INPUT INITIAL C AND DELTA C,OLD C,D=',2E10.4)
C
        READ(5,*) VAR(1,3),ENC
10      CN=CN
12      ICT=0
14      VAR(1,1)=VAR(1,2)
        VAR(1,2)=VAR(1,3)
        RES(1,1)=RES(1,2)
        RES(1,2)=RES(1,3)
        VAR(1,3)=VAR(1,3)+ENC
        ICT=ICT+1
        IF (ICT.GT.1000) GO TO 98
        C=VAR(1,3)
        CALL AGAR
C NOW COMPUTE THE RESIDUALS
        RES(1,3)=0.
        DO 5 I=1,K
        WN=(EPF(I)-TPF(I))
5       RES(1,3)=RES(1,3)+W(I)*WN*WN
```

64

```
C           WRITE(5,78) (VAR(1,J1),J1=1,3),(RES(1,J2),J2=1,3)
78          FORMAT(1X,'VAP,RES 1 TO 3 ARE:'6E10.4)
C IF LESS THAN 3 VALUES JUST CONTINUE.
            IF (ICT.LT.4) GO TO 14
C IF RES(1,2) IS LESS THAN RES(1,1) AND RES(1,3) THEN WE HAVE A MIN.
C SO CALCULATE WHERE MIN OCCURS, DROP ENC BY 10 AND CONTINUE.
            IF ((RES(1,2).LT.RES(1,1)).AND.(RES(1,2).LT.RES(1,3)))
           1GO TO 13
C IF RES(1,3).LE.RES(1,2) CONTINUE ELSE REVERSE ENC.
            IF (RES(1,3).LE.RES(1,2)) GO TO 14
            ENC=-ENC/2.
            GO TO 12
13          CALL MINI(1,VAR,RES,CN)
            WRITE(5,89) CN,RES(1,3)
89          FORMAT(1X,'CN AND RES(1,3) FOR THIS MIN ARE=',2E15.6)
            IF (ABS((CO-CN)/CN).LT.ERR) GO TO 111
            ENC=ENC/10.
            VAR(I,3)=CN
            GO TO 10
90          DO 81 I=1,K
            WRITE(5,79) (I,EPF(I),TPF(I),W(I))
79          FORMAT(1X,'I,EPF,TPF,W=',I2,3(1X,F13.6))
81          CONTINUE
            WRITE(5,310)
310         FORMAT(1X,'NOW INPUT SIG1,DELSIG1,NO OF DIVISIONS')
            READ(5,*) ST1,DST1,NOD
            DO 312 I=1,NOD+1
            F=0
            IF (ST1.LE.SIGU) GO TO 313
            Z=C*(ST1-SIGU)**EM
            F=1.-EXP(-Z)
313         WRITE(5,314) ST1,F
314         FORMAT(1X,'STRESS=',F10.5,' PROB=',F7.5)
            ST1=ST1+DST1
312         CONTINUE
98          WRITE(5,88) ICT
88          FORMAT(1X,'IMAX EXCEEDED, IMAX=',I6)
            GO TO 99
99          STOP
            END
            SUBROUTINE MINI(I,VAR,RES,XXX)
            DIMENSION VAR(3,3),RES(3,3)
            P1=RES(I,1)/((VAR(I,1)-VAR(I,2))*(VAR(I,1)-VAR(I,3)))
            P2=RES(I,2)/((VAR(I,2)-VAR(I,1))*(VAR(I,2)-VAR(I,3)))
            P3=RES(I,3)/((VAR(I,3)-VAR(I,1))*(VAR(I,3)-VAR(I,2)))
            AAA=P1+P2+P3
            BBB=P1*(VAR(I,2)+VAR(I,3))+P2*(VAR(I,1)+VAR(I,3))
           1 +P3*(VAR(I,1)+VAR(I,2))
            XXX=.5*BBB/AAA
            IF (VAR(I,1).GT.VAR(I,3)) GO TO 2
            IF ((XXX.GT.VAR(I,3)).OR.(XXX.LT.VAR(I,1)))
           1 XXX=(VAR(I,1)+VAR(I,3))/2.
            RETURN
2           IF ((XXX.GT.VAR(I,1)).OR.(XXX.LT.VAR(I,3)))
           1 XXX=(VAR(I,1)+VAR(I,3))/2.
            RETURN
            END
```

65

```fortran
      SUBROUTINE AGAR
      REAL L
      COMMON/PAR/K,L,C,T(40),FJ,SIGU,EM,RO,RI,TPF(40)
C COMPUTE DETERMINED PROBABLILTIES AT EACH TORQUE.
C STORE IN TPF(1 TO K).
C FIRST COMPUTE NECESSARY CONSTANTS.
      B=3.1416*2.*L*C/(EM+1.)
      DO 1 I=1,K
      TPF(I)=0.
      TIL=T(I)/FJ
C NOW COMPUTE R AT WHICH THE THRESHOLD STRESS OCCURS.
      RLOW=RI
      RTH=SIGU/TIL
      IF (RTH.GE.RO) GO TO 1
      IF (RTH.GT.RI) RLOW=RTH
C NOW COMPUTE BN.
      C1=RO*TIL
      C2=(C1-SIGU)**(EM+1.)
      C3=C2*(C1-SIGU)
      D1=RLOW*TIL
      D2=(D1-SIGU)**(EM+1.)
      D3=D2*(D1-SIGU)
      BN=B*((RO*C2-C3/(TIL*(EM+2.)))-
     1  (RLOW*D2-D3/(TIL*(EM+2.))))/TIL
      TPF(I)=1.-EXP(-BN)
    1 CONTINUE
      RETURN
      END
```

NO OF COPIES

Commander   9
Naval Air Systems Command
Washington, DC 20361
Attention: AIR-OOD4   6
          AIR-310A   1
          AIR-5304C1   2

Office of Naval Research   1
800 N. Quincy Street
Arlington, VA 22217
Attention: Code 471

Commander   1
Naval Surface Weapons Center
White Oak
Silver Spring, MD 20910
Attention: Code R31

Director   1
Naval Research Laboratory
Washington, DC 20375
Attention: Code 6360

Commanding Officer   1
David W. Taylor Naval Ship Research & Development Center
Annapolis, MD 21412
Attention: W. Smith, Code 2832

Commander   2
Air Force Wright Aeronautical Laboratories
Wright-Patterson Air Force Base
Dayton, OH 45433
Attention: Dr. J. Dill   POSL 1
          Dr. H. Graham   MLLM 1

Brookhaven National Laboratory   1
Upton, NY 11973
Attention: Dr. D. Van Rooyen

Director   1
Applied Technology Laboratory
US Army Research & Technology Laboratories
Fort Eustis, VA 23604
Attention: DAVOL-ATL-ATP (Mr. Pauze)

US Army Research Office   1
Box CM, Duke Station
Durham, NC 27706
Attention: CRCARD

	NO OF COPIES
Army Materials and Mechanics Research Center Watertown, MA 02172 Attention: Dr. R. N. Katz	1
NASA Headquarters Washington, DC 20546 Attention: C. F. Bersch, RTM-6	1
NASA Lewis Research Center 21000 Brookpark Road Cleveland, OH 44135	2

NASA Lewis Research Center   2
21000 Brookpark Road
Cleveland, OH 44135
Attention: Dr. E. Zaretsky   1
           W. A. Sanders (49-1)   1
                and Dr. T. Hergel

Defense Advanced Research Project Office   1
1400 Wilson Blvd
Arlington, VA 22209
Attention: Dr. Van Reuth

Inorganic Materials Division   1
Institute for Materials Research
National Bureau of Standard
Washington, DC 20234

Department of Engineering   1
University of California
Los Angeles, CA 90024
Attention: Profs. J. W. Knapp and G. Sines

Engineering Experiment Station   1
Georgia Institute of Technology
Atlanta, GA 30322
Attention: J. D. Walton

University of Illinois   1
College of Engineering
204 Ceramics Building
Urbana, IL 61801
Attention: Sherman D. Brown
           Department of Ceramic Engineering

Department of Engineering Research   1
North Carolina State University
Raleigh, NC 27607
Attention: Dr. H. Palmour

Ceramic Science and Engineering Section   1
Pennsylvania State University
University Park, PA 16802
Attention: Dr. R. E. Tressler

Rensselaer Polytechnic Institute   1
110 Eighth Street
Troy, NY 12181
Attention: R. J. Diefendorf

	NO OF COPIES
School of Ceramics Rutgers, The State University New Brunswick, NJ 08903	1
Virginia Polytechnic Institute Minerals Engineering Blacksburg, VA 20460 Attention: Dr. D. P. H. Hasselman	1
Advanced Mechanical Technology Inc. 141 California Street Newton, MA 02158 Attention: Dr. Walter D. Syniuta	1
Aerospace Corporation Materials Laboratory P.O. Box 95085 Los Angeles, CA 90045	1
Batelle Memorial Institute 505 King Avenue Columbus, OH 43201 Attention: Ceramics Department 1 Metal & Ceramic Information Center 1	2
Research and Development Division Carborundum Company Niagra Falls, NY 14302 Attention: Mr. C. McMurty	1
Ceramic Finishing Company Box 498 State College, PA 16801	1
Ceradyne Inc. Box 1103 Santa Ana, CA 92705	1
Coors Porcelain Company 600 Ninth Street Golden, CO 80401 Attention: Research Department	1
Federal-Mogul Corporation Anti-Friction Bearing R&D Center 3980 Research Park Drive Ann Arbor, MI 48104 Attention: D. Glover	1
Metallurgy and Ceramics Research Department General Electric R&D Laboratories P.O. Box 8 Schenectady, NY 12301	1

Hughes Aircraft Company   1
11940 W Jefferson Boulevard
Culver City, CA 90230
Attention: M. N. Gardos
M S D 133-Bldg. 6

IIT Research Institute   1
10 West 35th Street
Chicago. IL 60616
Attention: Ceramics Division

Kaweki-Berylco Industry   1
Box 1462
Reading, PA 19603
Attention: Mr. R. J. Longnecker

Research & Development Division   1
Arthur D. Little Company
Acorn Park
Cambridge, MA 02140

Mechnaical Technology, Inc.   1
968 Albany-Shaker Road
Latham, NY 12110
Attention: Dr. E. F. Finkin

Norton Company   1
Industrial Ceramics Division
One New Bond Street
Worchester, MA 01606
Attention: Dr. M. Torti

Ceramic Division   1
Sandia Corporation
Albuquerque, MN 87101

SKF Industries Inc.   1
1100 First Street
P. O. Box 515
King of Prussia, PA 19406
Attention: P. A. Madden

Southwest Research Institute   1
P. O. Drawer 28510
San Antonio, TX 78228

Materials Sciences & Engineering Laboratory   1
Stanford Research Institute
Menlo Park, CA 94025
Attention: Dr. Cubiciotti

Teledyne CAE   1
1330 Laskey Road
Toledo, OH 43601
Attention: Hugh Gaylord

Union Carbide Corporation   1
Parma Technical Center
P. O. Box 6116
Cleveland, OH 44101

Materials Sciences Laboratory   1
United Technologies
East Hartford, CT 06101
Attention: Dr. J. J. Brennan

United Technologies Research Center 1
East Hartford, CT 06108
Attention: F. L. Ver Snyder   .

Astronuclear Laboratory   1
Westinghouse Electric Corporation
Box 10864
Pittsburgh, PA 15236

Westinghouse Research Laboratories 1
1310 Beulah Road
Churchill Borough
Pittsburgh, PA 15235
Attention: Dr. R. Bratton

Richard W. Perkins, Jr.   1
Professor and Chairman,
Department of Mechanical
 and Aerospace Engineering
139 E. A. Link Hall
Syracuse, N. Y. 13210

Ms. Janice Fleming, Managing Editor
I & E Product R/D
American Chemical Society
1155 16th Street, N.W.
Washingtion, D. C. 20036   1